

PMP Inter-laboratory Correlation Exercise



Report on PART 3: JRC Tests in July'06

Prepared by

Barouch Giechaskiel, Rafael Muñoz-Bueno, Rinaldo Colombo, Urbano Manfredi
Panagiota Dilara

PMP Inter-laboratory Correlation Exercise Report on PART 3: JRC Tests in July'06

Transport and Air Quality Unit
Institute for Environment and Sustainability
EC Joint Research Centre, Ispra

Barouch Giechaskiel, Rafael Muñoz-Bueno, Rinaldo Colombo, Urbano Manfredi
and Panagiota Dilara,

Mission Statement: The mission of the Institute for Environment and Sustainability is to provide scientific-technical support to the European Union's Policies for the protection and sustainable development of the European and global environment.

LEGAL NOTICE

Neither the European Commission nor any person acting on behalf of the Commission is responsible for the use which might be made of the following information.

A great deal of additional information on the European Union is available on the Internet. It can be accessed through the European server (<http://europa.eu.int>)

Content

1. INTRODUCTION	1
2. EXPERIMENTAL METHODS	2
CYCLES & STEADY STATE TESTS	2
TEST VEHICLE	4
FUEL AND LUBE OIL	5
SAMPLING SYSTEMS AND CONDITIONS	5
Dilution air	5
Dilution tunnel	5
PM sampling	6
Particle number sampling	7
Instrumentation	7
GASEOUS POLLUTANTS	8
TEST PROTOCOL	8
Cold NEDCs	8
Regeneration NEDCs	9
3. RESULTS	10
PHASE #3 RESULTS	10
Valid tests	10
Legislated emissions	11
Regeneration and -7 °C test	12
Particle number emissions	12
Real time PN emissions	13
Mass comparisons	15
VEHICLE SOAKING AND PRECONDITIONING EFFECT	16
OTHER DRIVE CYCLES	18
OLD AND NEW BACKGROUND	19
Background Particle Mass Levels and Limit of Detection	20
PMP AND LEGISLATED PM METHODS	21
Single vs. Multiple and Backup Filter Effects	21
Cyclone and Filter Heating Effects	21
Filter Media Effects	23
BEFORE-AFTER REGENERATION	24
REGENERATION EMISSIONS	25
Size distributions	27
Regeneration during steady state tests	29
DPF STABILIZATION	31
COMPARISON OF THE THREE PHASES	32
4. DISCUSSION & CONCLUSIONS	35
PHASE #3 RESULTS	35



EXTRA MASS TESTS.....	35
PARTICLE NUMBER EMISSIONS.....	35
Cold Start emissions.....	35
Before-After regeneration	35
During regeneration	36
Stabilization times.....	36
PM suitability.....	36
COMPARISON OF THREE PHASES.....	37
<i>References.....</i>	<i>38</i>
<i>DEFINITIONS, ACRONYMS, ABBREVIATIONS</i>	<i>39</i>
<i>ANNEXES</i>	<i>42</i>
Annex A. Test fuel specifications for the Golden Vehicle	42
Annex B. Third phase of measurements in JRC.....	43

List of Figures

Figure 1: New European Driving Cycle (NEDC) and its two phases i) urban (ECE) and ii) Extra-Urban (EUDC).	2
Figure 2: a) Urban b) Road c) Motorway parts of the ARTEMIS cycle (CADC). Arrows indicate the sampling times. However these times were not taken into account and PM samples were taken during the whole duration of the cycles.	3
Figure 3: The golden vehicle: Peugeot 407 - Saloon 2.0 Hdi 136 SE	4
Figure 4: Set up.	6
Figure 5: Non valid measurements and outliers in the third phase.	10
Figure 6: Gaseous emissions of valid tests. Error bars show 2 standard deviations.	11
Figure 7: Gaseous and PM emissions during a non-regenerating, a regenerating and a -7°C NEDC.	12
Figure 8: Particle Number (PN) and Particulate Matter (PM) emissions. Error bars show 2 standard deviations.	13
Figure 9: Non-volatile and total NEDC particle number concentration measured over an NEDC cycle. The arrows indicate the time that the size distribution of Figure 12 correspond.	13
Figure 10: Relative concentration of particles over the NEDC for the data of Figure 9.	14
Figure 11: Real-time Emissions of Carbon from the Golden vehicle by LII (data from NTSEL).	14
Figure 12: Cold start at 32 km/h (15 s average) size distribution measured with the EEPS (total particles) at the time indicated by an asterisk in Figure 9.	15
Figure 13: Comparison of mass results with different methods.	16
Figure 14: Effects of Vehicle Preconditioning and Soaking on Particulate Mass Emissions	17
Figure 15: Effects of Vehicle Preconditioning on Particle Number Emissions	17
Figure 16: Comparative Cold and Hot NEDC, ECE & EUDC Particle Number Emissions (with no preconditioning).	18
Figure 17: Particulate Mass Emissions Different Cycles.	18
Figure 18: Particle Number Emissions – Various Emissions Cycles	19
Figure 19: Comparison of Background PM and LOD with Sample PM.	20
Figure 20: Comparison of Background Particle Number and LOD with Lab#3 Data	20
Figure 21: Effect on PM emissions of different filter configurations.	22
Figure 22: PN emissions stability during the filter mass measurements of Figure 21.	22
Figure 23: Effects of cyclone and system heating on mass emissions.	22
Figure 24: PN emissions stability during the filter mass measurements of Figure 23.	23
Figure 25: Comparison of mass emissions with 2 different filter media.	23
Figure 26: Particle Number emissions and background during filter media tests of Figure 25.	24
Figure 27: Non-volatile particle number concentration over NEDC before and after a regeneration event (with standard preconditioning).	24
Figure 28: Total and non-volatile particle emissions during a regenerating cycle.	25
Figure 29: a) Particle number emissions over EUDCs. b) PM emissions over NEDCs before, during and after regeneration events. Bigger points with black foreground line correspond to cold start NEDCs. Smaller points are hot start NEDCs.	26
Figure 30: Particle number size distributions during regeneration events where NM appeared a) during the acceleration of 70 to 100 km/h b) during 100 km/h c) during 70 km/h. Each size distribution corresponds to 1 second of measurements. The exact times of the measurements are shown at the bottom of the figure.	28
Figure 31: Particle number emissions by CPCs during 120 km/h cruise.	29
Figure 32: Particle number emissions by CPCs during 120 km/h active regeneration.	30
Figure 33: Particle emissions during passive regeneration at 140 km/h.	30
Figure 34: Particle emissions during steady state regenerations.	31
Figure 35: Stabilization distance after regeneration events.	32
Figure 36: CO ₂ emissions at the three JRC phases.	33
Figure 37: CO emissions at the three JRC phases.	33
Figure 38: NO _x emissions at the three JRC phases.	33
Figure 39: HC emissions at the three JRC phases.	34
Figure 40: PM emissions at the three JRC phases.	34

Figure 41: Particle number emissions at the three JRC phases. 34

Figure 42: Particle number emissions before, during and after a regeneration. The contribution of ECE and EUDC emissions is given with a horizontal line which is calculated by simply dividing ECE or EUDC emissions [in km⁻¹] with the sum of ECE and EUDC emissions [in km⁻¹]. 36

List of Tables

Table 1: Diesel DPF (FBC) technical information. 4

Table 2: Fuel specifications. 5

Table 3: Specifications of dilution air system. 5

Table 4: Regulated gaseous emissions specifications. 8

Table 5: Third period of measurements in JRC. 9

Table 6: PM and Number results for JRC Phase #3. 11

Table 7: Vehicle's Regulated Emissions - Compliant With Euro 4. 12

Table 8: Various Vehicle Preconditionings and Soakings. 16

Table 9: Old and new background levels. 19

Acknowledgments

The authors would like to gratefully acknowledge Jon D. Andersson from RICARDO, who acted as the Golden Engineer for the PMP Intercomparison Exercise, for his helpful advice throughout and following the testing . We would also like to thank Giorgio Martini for his expertise and technical advice which were a great support for the investigators. And at last but not the least, we would like to thank Gaston Lanappe, Philippe Le Lijour and Mirco Sculati for their excellent hard work and long hours put in during the tests in the laboratory.

1. INTRODUCTION

This document reports the results of the third part of the testing performed during the PMP inter-laboratory exercise - 13 July to 18 August 2006 - conducted at the Vehicles Emissions Laboratory (VELA2) in the Transport and Air Quality Unit of the European Commission's Joint Research Centre (JRC-Ispra). This report presents the results of the work undertaken on a 2.0 HDi diesel car equipped with a Diesel Particulate Filter (DPF), i.e. the *Golden Vehicle*. Most of the tests complied with all the requirements of the document UN-GRPE PMP Phase 3. Inter-laboratory Correlation Exercise: Framework and Laboratory Guide. The measurements included both filter based particulate mass measurements and real-time particle number measurements performed under transient conditions on a chassis dynamometer. Extra tests were conducted in order to investigate the effect of the PMP recommendations over the legislated procedures (filter media, temperature, cyclone, no backup filter). Moreover the regeneration emissions were investigated. Finally comparisons with the previous measurements of the same vehicle in JRC were made.

2. EXPERIMENTAL METHODS

In the following sections the experimental details for the measurements conducted in the JRC facilities will be described.

CYCLES & STEADY STATE TESTS

The standard New European Driving Cycle (NEDC) emissions certification test for light duty vehicles was used (Figure 1). This cycle has been used in Europe for certification of light duty vehicles since 2000 and consists of the urban part (ECE) and the extra urban part (EUDC). In order to improve the readability of the figures at the results section of this paper the pattern of the cycle is not shown. In addition, three real-world driving cycles which were developed in the framework of the ARTEMIS project [1] were measured (Figure 2). These cycles were developed by statistical analysis of speed profile databases consisting of 90 000 km monitored on board 80 passenger cars in France, Germany, Great Britain and Greece, supplemented by another 10 000 km obtained in Switzerland and Italy under controlled traffic conditions. These cycles, named Common Artemis Driving Cycles (CADC) by convention, correspond to total of 40 minutes of urban, rural and motorway driving which describe a range of representative driving conditions encountered in Europe. Arrows in the Figure indicate the prescribed PM sampling times. However these times were not taken into account and PM samples were taken during the whole duration of the cycles, due to difficulties in the dilution tunnel control software. A number of limited steady state tests at 120 and 140 km/h were conducted in order to investigate the regeneration emissions of the vehicle.

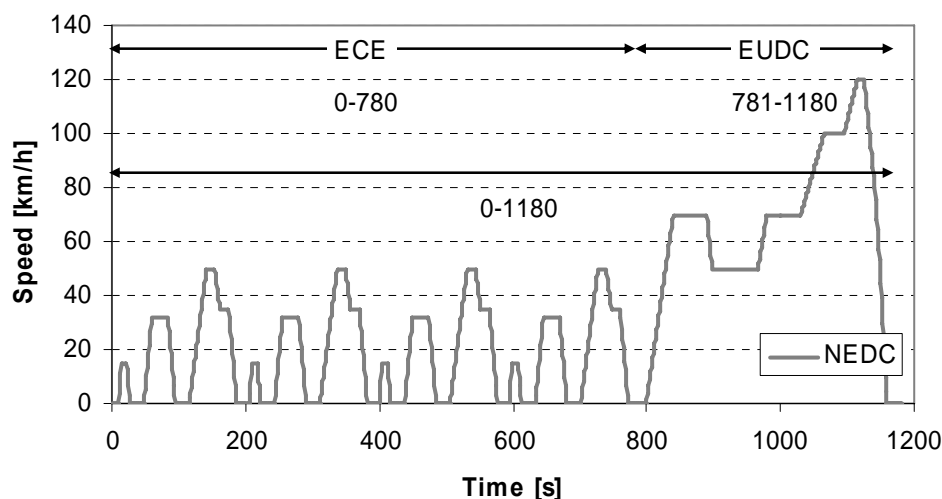


Figure 1: New European Driving Cycle (NEDC) and its two phases i) urban (ECE) and ii) Extra-Urban (EUDC).

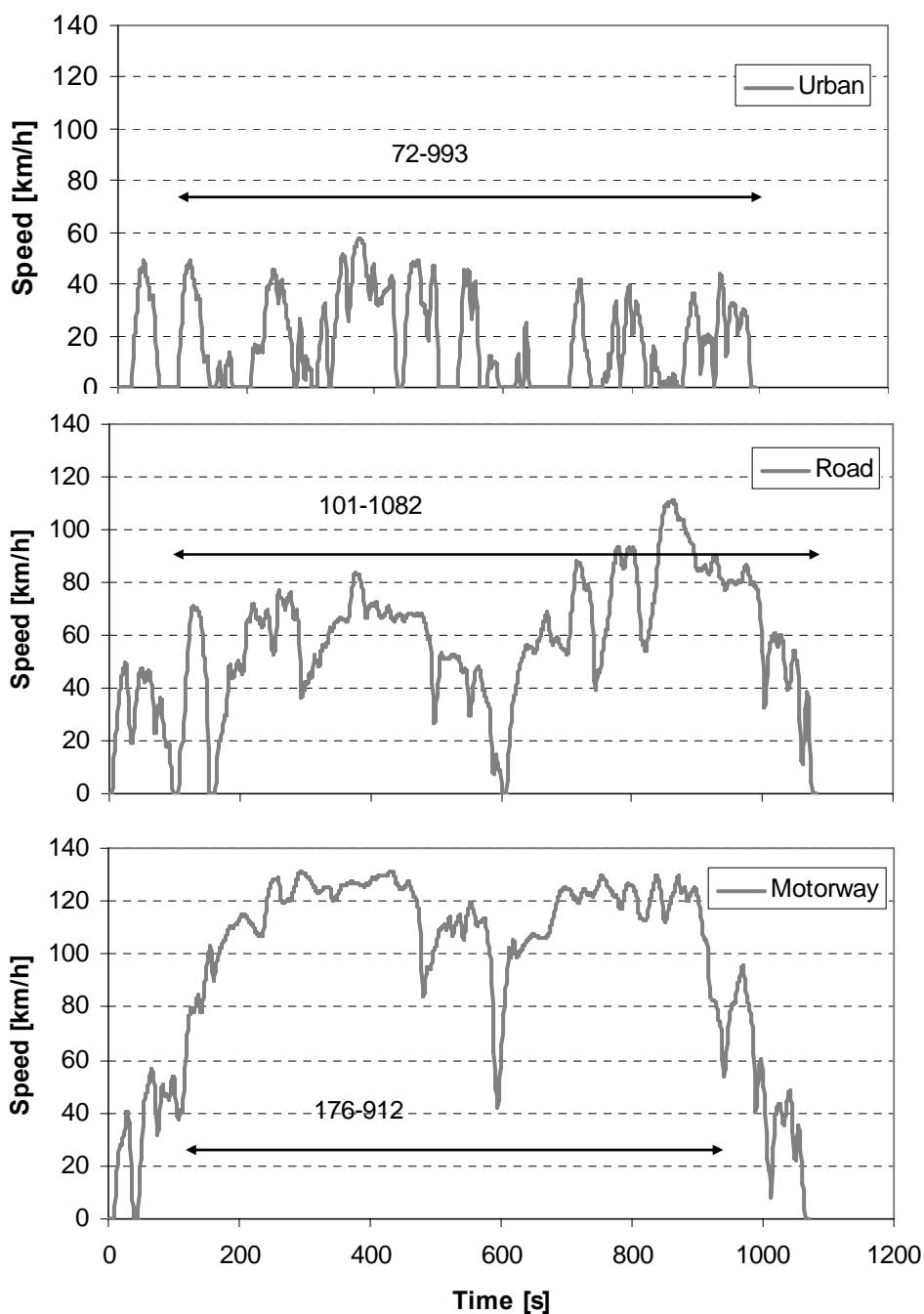


Figure 2: a) Urban b) Road c) Motorway parts of the ARTEMIS cycle (CADC). Arrows indicate the sampling times. However these times were not taken into account and PM samples were taken during the whole duration of the cycles.

TEST VEHICLE

The vehicle used in this study (Figure 3) was the PMP “golden car”, i.e. a Peugeot 407 HDi FAP (Filtre à Particules) type that represents the most mature Diesel Particulate Filter (DPF) technology present on the market and was fully Euro 4 compliant. The Peugeot 407 is a turbocharged common rail direct injection Diesel vehicle (Table 1) equipped with a FAP Aftertreatment system. This FAP system employs an oxidation catalyst upstream of an uncoated Silicon Carbide wall-flow DPF plus cerium based fuel borne catalyst (FBC) to reduce the regeneration temperature. It also uses post-injection and Engine Gas Recirculation (EGR) shut-off to generate an exotherm when periodically regenerating the DPF. The mileage of the vehicle at the beginning of the experiments was 17605 km. The vehicle was offered by the AECC to the PMP programme for use during the PMP light-duty inter-laboratory validation exercise.

Table 1: Diesel DPF (FBC) technical information.

Vehicle Model/Reg.	Peugeot 407 – Saloon 2.0 Hdi 136 SE
No. Of Cylinders	4
Aspiration	Turbocharged
2 or 4 Stroke	4
Fuel Delivery	Common rail D.I.
Capacity (cc)	1997
Test Inertia (lbs)	3500
Kerb Weight (kg)	1590
Transmission	6 speed manual
Aftertreatment #1	Oxidation Catalyst
Aftertreatment #2	Si-C DPF



Figure 3: The golden vehicle: Peugeot 407 - Saloon 2.0 Hdi 136 SE

FUEL AND LUBE OIL

The lubricating oil used was provided by Castrol, offered by CONCAWE as support to the PMP light-Duty Inter-laboratory Exercise. The test lubricant was a fully synthetic, 0W/40 PAO (polyalphaolefin) based oil with <0.2% sulfur content. The vehicle was conditioned with the fresh lubricant by driving a distance of 500 km.

The only fuel used in this vehicle, which was provided by CONCAWE again for the PMP exercise, complied with Annexes 3 and 4 of Directive 2003/17/EC describing fuel specifications to be employed after 1st January 2009 (i.e. sulfur content of lower than 10 ppm). The most important properties can be seen in Table 2 and detailed specifications in Annex A.

Table 2: Fuel specifications.

<i>Properties</i>	<i>Units</i>	<i>Value</i>
Cetane Number	[-]	53
Density	[kg/m ³]	835
Sulfur	[ppm]	8
Polycyclic aromatics	[%]	4.4

SAMPLING SYSTEMS AND CONDITIONS

Sampling was conducted according to the current legislation and the proposals of the Particle Measurement Programme (PMP) [2]. The measurements were done on a 48" 4x4 dynamometer MAHA SN 87 (roller diameter of 1.220 m and 150 kW) at the JRC laboratories (VELA 2).

Dilution air

Following the PMP recommendations, the exhaust was primarily diluted and conditioned following the CVS procedure. Highly efficient dilution air filters for particles and hydrocarbons that reduce particle contributions from the dilution air to near zero were used (99.99% of reduction for particles with size diameter of 0.3 μ m) (Table 3). The temperature of the dilution air and the relative humidity were conditioned to 23 \pm 1°C and 50 \pm 5% relative humidity. The dilution air conditioning and filtering system was new (different than during the first and second phases of measurements in JRC). During the measurement campaign it was found that the dilution system didn't operate correctly, so some measurements had to be disregarded. More details in [3].

Table 3: Specifications of dilution air system

<i>Type</i>	<i>Model</i>	<i>Efficiency</i>	<i>Flow [m³/h]</i>	<i>ΔP [Pa]</i>
Particle Filter	3QMHF242412-90	85/90-F7 CEN EN 779	2000	50
Active Charcoal	CAMCARB 1000-CM05		2000	40
Particle Filter	SOLIFAIR 1560.02	H13-N1822 : 99.99 @ 0.3 μ m	2000	120

Dilution tunnel

It should be also noted that according to the PMP Interlab Guidance Document the vehicle was coupled to the CVS transfer line by a metal-to-metal joint during testing to avoid the possibility of exhaust contamination by the high-temperature breakdown of elastomer coupling elements. The exhaust was transported to the tunnel through a 9 m long heated at 70°C corrugated stainless steel tube. It was

introduced along the tunnel axis, near an orifice plate that ensured rapid mixing with the dilution air. The flow rate of dilute exhaust gas through the tunnel was controlled by a critical orifice venturi. A flowrate of 12 m³/min at standard reference conditions (20°C and 1 bar) was used in the measurements. The tunnel operated in the turbulent flow regime ($Re = 53\,500$). Based on standard reference flowrates, the mean dilution ratio achieved in the CVS was 12.2:1 at 32 km/h (2nd gear), 12.5:1 at 50 km/h (3rd gear), 15.1 at 70 km/h (5th gear), 8.3:1 at 100 km/h (5th gear) and 5.6:1 at 120 km/h (5th gear). The residence time of the exhaust in the dilution tunnel was 1.3 s.

The schematic of the set up can be seen in Figure 4. Two different probes were used for sampling, placed at the same cross-section of the tunnel and facing upstream the flow. One probe was used for PM measurements and the other for particle number (PN). These probes were installed 10 tunnel diameters downstream of the mixing point to ensure complete mixing of the dilution air and the exhaust gas.

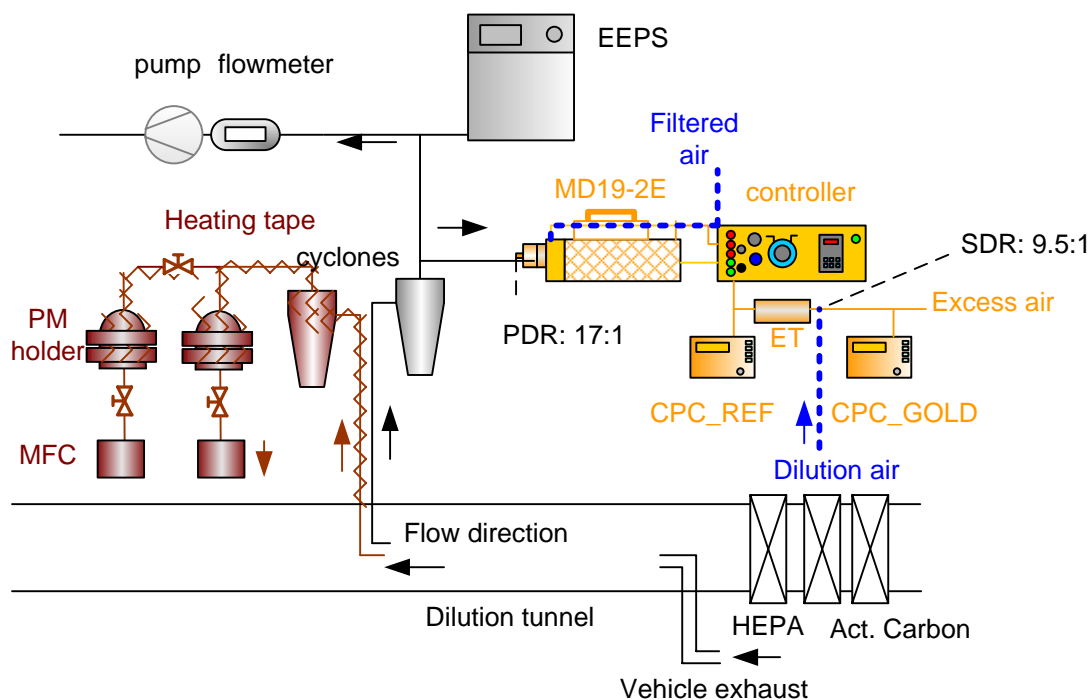


Figure 4: Set up.

PM sampling

An improved mass measurement procedure was used according to PMP recommendations. PM samples were drawn directly from the CVS at a constant flowrate of 50 lpm at normal conditions (0°C and 1 bar) for all the experiments to improve repeatability. A cyclone pre-classifier (URG-2000-30EP) with a 50% cut-size at 4 μm (for a flowrate of 50 lpm) was used to limit the contribution of reentrained and wear materials to the filter mass.

The filter holder and transfer tubing were externally heated by direct surface heating to permit aerosol stabilization of >0.2 s prior to sampling and to ensure close control of the filter face temperature to 47°C ($\pm 5^\circ\text{C}$).

PM samples were collected on 47 mm Teflon-coated glass-fiber Pallflex® TX40H120-WW filters. One single 47 mm filter was used rather than primary and back-up filters to eliminate weighing errors and the

volatile artifacts of the back-up filter. For the same reasons one filter was used for the entire NEDC rather than separate urban (ECE) and extra-urban (EUDC) phases. To quantify this artifact effect some tests were conducted with two filters (one for the ECE and one for the EUDC part of the cycle) and some other tests with two filters for the whole NEDC cycle (main and backup filters for the whole NEDC cycle). Some extra tests were conducted with Teflo Membrane filters in order to compare the effect of volatile artifact depending on the material of the filter reported by various investigators.

Filters were kept in a controlled temperature and humidity chamber ($22\pm 1^\circ\text{C}$ and $50\pm 5\%$, respectively) and they were weighted with a Mettler Toledo model UMX2 balance (sensitivity 10^{-7} g) before and after the measurement, allowing at least 2 hours for conditioning. Electrostatic charge effects were minimized by the use of HAUG Type EN SL LC 017782100 neutralizer and grounded conductive surfaces. Each filter was weighted at least three times, and the average of the weightings was used in calculating mass changes.

Particle number sampling

Aerosol samples for particle number measurement were drawn from the CVS with a constant flowrate of 90 lpm (Figure 4). A cyclone pre-classifier (URG-2000-30EP) with a 50% cut-size at $2.5\ \mu\text{m}$ (for a flowrate of 90 lpm) was used.

A MD19-2E rotating disk dilutor (Matter Engineering AG) with short (~ 0.1 m) not heated sampling line of stainless steel was sampling downstream the cyclone. Particle losses inside the short sampling tube (upstream of the sampling device) are calculated at 2% for 10 nm particles and zero for 100 nm particles.

In this study the 10 cavity disk was used and the rotation frequency was set to 65% leading to a Dilution Ratio (DR) of 17:1 (initially it was used 19.65 by mistake, but all results shown here have been corrected) according to the recent manufacturer's calibration. The temperature was set to 150°C for both the dilutor body and dilution air in order to evaporate volatile particles and reduce the partial pressures of the gas phase species to prevent recondensation at the dilutor exit. However, the dilution air was possible to reach only 120°C as indicated by the lamp on the unit's controller, but this temperature was high enough for the evaporation of volatiles and to avoid condensation of water.

The temperature of the evaporation tube was set at 300°C ($\pm 1^\circ\text{C}$) in order to evaporate all volatiles and semi-volatile compounds. The residence time in this tube was 0.2 s. The penetration for solid particles was more than 80% and the evaporation efficiency of $n\text{-C}_{40}\text{H}_{82}$ particles with diameter of 30 nm and concentration of at least $1000\ \text{cm}^{-3}$ was more than 99% according to the manufacturer.

Immediately downstream of the evaporation tube there was a simple air mixer dilutor in order to minimize the diffusion losses, cool the hot diluted exhaust gas and reduce the particle number concentration below $10^4\ \text{cm}^{-3}$ in order to be within the detection limit of the CPC. The dilution ratio was constant 9.5:1 for the specific flowrates in this set up.

Instrumentation

Two 3010D Condensation Particle Counter (CPC) (TSI inc.) were used for the measurements. The CPCs were calibrated before the measurements and had a controlled counting efficiency curve with $d_{50\%}$ at 23 nm. The strictly controlled counting efficiency curve was considered necessary to exclude the possible measurement of a nucleation mode present below 20 nm while including the primary carbon sphere size of ~ 20 nm. A 0.1 m long tube connected one CPC downstream the dilution device (after the second dilutor) with an estimated 2% losses for 10 nm particles. This CPC was considered to measure non-volatile particles. The other CPC was connected upstream the evaporation tube in order to measure semi-volatile (and non-volatile) particles.

A 3090 Engine Exhaust Particle Sizer Spectrometer (EEPS) (TSI Inc.) was used for a limited number of tests (11 Regeneration NEDC tests, as it will be explained in the test protocol section). EEPS measured particle size distribution with a maximum data rate of 10 size distributions per second (although averages of 1 s were used in the graphs of this study). It measured particle sizes from 5.6 to 560 nm with a sizing resolution of 16 channels per decade (a total of 32 channels). At the instrument's inlet there was a cyclone with a 50% cut-size at 1 μm (inlet flowrate 10 lpm). By integrating the size distribution the total particle number concentration could be estimated. As the instrument was directly connected to CVS through the particle number sampling probe it was considered that it measured volatiles and non-volatile particles >6 nm (called total particles by convention). Moreover, it was possible to estimate the contribution of volatile (and semi-volatile) particles by comparing the CPC downstream (or upstream) the evaporation tube with the EEPS. It must be noted here that the existence of non-volatile particles $<22\text{nm}$ cannot be excluded and this is discussed in the text whenever volatility of NM is hypothesised in the text. EEPS and CPCs were not inter-calibrated but the expected divergence in their common size range is expected to be less than 20% [4].

GASEOUS POLLUTANTS

The gaseous emissions were measured during cold NEDCs in accordance with the current R83 regulation. A Horiba MEXA-7400HTR-LE instrument was used for CO, HC, NO_x and CO₂ measurements. Total HC emissions were measured by heated flame ionization detector (FID). The CO and CO₂ emissions were determined by non-dispersive infra-red analyzers and NO_x were measured using a chemiluminescence analyzer. The technical specifications are shown in Table 4.

Table 4: Regulated gaseous emissions specifications.

Model	HORIBA MEXA – 7400 HTR LE
THC	FID: FIA 726LE
CO	NDIR: AIA 721A
CO ₂	NDIR: AIA 772
NO _x	CLA 750 LE

TEST PROTOCOL

For the whole period of the measurements (2 months) only the particular vehicle was tested in the laboratory, therefore no artifacts due to released material from other vehicles or fuels are expected.

Cold NEDCs

However, in order to minimize any desorption/release phenomena that have been reported [5] a standard preconditioning was performed on the days before a cold start NEDC test. It consisted of the legislated Diesel conditioning (3 x EUDC), preceded by a 120 km/h steady state cruise of 20 minutes duration. This 120 km/h steady state raised the temperature of the vehicle's exhaust system, transfer tube to the CVS and CVS tunnel to a level above that experienced during a standard NEDC test. This purged the exhaust and transfer system of materials that may have contaminated the test result, especially at such low levels of PM emissions, and ensured that any small contribution from the 3 x EUDC cycle conditioning would be replicated exactly from test-to-test, thus reducing variability. After the 3 x EUDC conditioning was complete, the CVS tunnel was left running for 15 min with the vehicle still attached to enable materials released from the exhaust and sampling system during cooling to be drawn

away. For some tests the preconditioning was different (e.g. 10 min at 120 km/h and 1 x EUDC, or 15 min at 130 km/h or 15 min idle) in order to investigate the effect of the pre-conditioning on particle number emissions.

After the preconditioning, the vehicle was left to cool for at least 6 hours (soaking) before the beginning of another measurement (maximum two measurement per day). The temperature of the test facilities was always 23°C except for one test (-7°C), which will be examined separately.

Regeneration NEDCs

For a number of tests (around 11 NEDCs – one week of measurements) no standard preconditioning was done in between the cycles in order to catch/observe the regeneration of the vehicle during the normal NEDC tests. Moreover, in most of these tests the vehicle soaking was from a few minutes to a few hours. In order to distinguish these tests from the rest NEDC cycles, these NEDC tests are called “NEDC Regeneration tests”.

Table 5 gives the general overview of the measurements conducted at the third phase of the JRC measurements. A detailed plan of the measurements can be seen in Annex B.

Table 5: Third period of measurements in JRC.

9 Jun – 13 Jun	Steady State regeneration tests	Active-Passive
14 Jun – 26 Jun	First series of measurements	New filtering system. Not working properly
3 Jul – 14 Jul	NEDC Regeneration tests	No preconditioning/soaking
19 Jul – 8 Aug	Extra mass tests	Old background
9 Aug – 18 Aug	Teflo, CADC	New background

3. RESULTS

In the following sections the results of the measurement campaign are presented. Data are not corrected for any particle losses. In most figures only one test is reported to improve the readability of the figures, as all other tests showed similar results. Emissions that are reported in [km⁻¹] refer to tailpipe conditions and concentrations given in [cm⁻³] refer to the CVS. However they can be easily converted to tailpipe concentration using the dilution ratios reported in the “Sampling systems and conditions” section. When more than one measurement is reported, then the average value is given. In this case, the ratio of the standard deviation of the measurements to the average value of the measurements, the Coefficient of Variance (CoV) is sometimes referred as *repeatability* of the measurements. Error bars show one standard deviation.

PHASE #3 RESULTS

Valid tests

The valid Particulate Matter (PM) and Particle Number (PN) results of the third phase can be seen in Table 6. Only the tests according to the protocol are shown here. The extra tests conducted for the investigation of the system and the regeneration effect will be reported separately. It should be noted here that the first tests (#1-#10) had high PM emissions. It is believed that this was due to the wrong operation of the new dilution tunnel dilution air system installed (see paragraph “Old and new Background” and [3]). So these tests are considered non valid. From the rest tests, one was considered as an outlier according to the PM criterion (Figure 5).

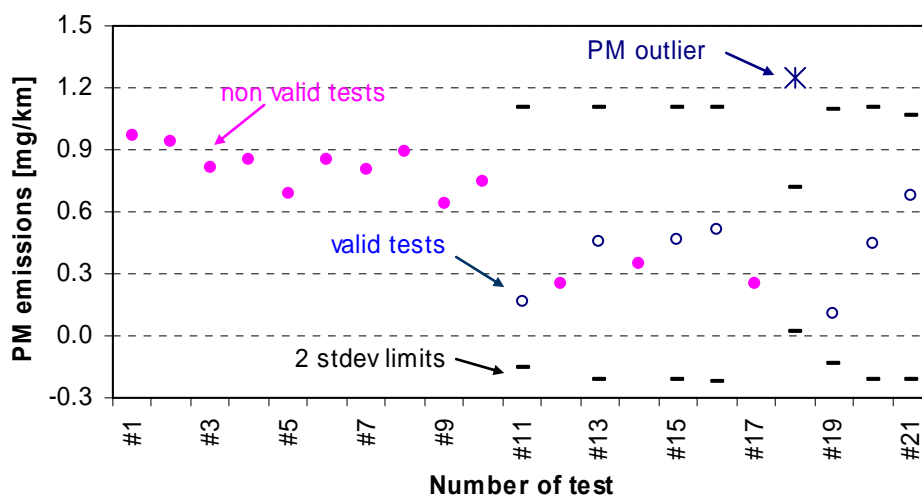


Figure 5: Non valid measurements and outliers in the third phase.

It should be reminded that in this inter-laboratory exercise [2], a test (including all emissions) was considered to be an outlier when its PM result lay outside 2 standard deviations of the *rest* of that laboratory’s PM measurements. The PM results were only considered for the identification of an outlier since filter based mass was considered to be the reference method. It is clear that this criterion tunes the dataset to the best quality particulate mass results.

Table 6: PM and Number results for JRC Phase #3.

Dates	GPMS NEDC [#/km]	PM NEDC [mg/km]	PM valid tests	Comment
13-June-06	4.67E+10	0.963	non valid test	Installation
14-June-06	1.58E+11	0.937	non valid test	
15-June-06	9.86E+10	0.809	non valid test	
16-June-06	6.64E+10	0.855	non valid test	
19-June-06	4.49E+10	0.683	non valid test	
20-June-06	4.55E+10	0.853	non valid test	
21-June-06	5.12E+10	0.808	non valid test	
22-June-06	3.88E+10	0.893	non valid test	
23-June-06	6.89E+10	0.635	non valid test	
26-July-06	8.31E+10	0.744	non valid test	
26-July-06	8.46E+10	0.160	valid test	
26-July-06	1.60E+10	0.252	non valid test	Different precond.
27-July-06	1.28E+11	0.450	valid test	
27-July-06	2.02E+10	0.344	non valid test	Different precond.
28-July-06	9.38E+10	0.461	valid test	
31-July-06	7.24E+10	0.510	valid test	
31-July-06	9.82E+09	0.254	non valid test	Different precond.
8-Aug-06	1.30E+11	1.246	PM non valid test	
9-Aug-06	9.32E+10	0.106	valid test	
11-Aug-06	1.36E+11	0.446	valid test	
18-Aug-06	8.32E+10	0.679	valid test	

Legislated emissions

The results of the gaseous emissions of the “valid” tests are shown in Figure 6. They are consistent with the expected levels quoted for the test vehicle by the UK Vehicle Certification Agency (Table 7).

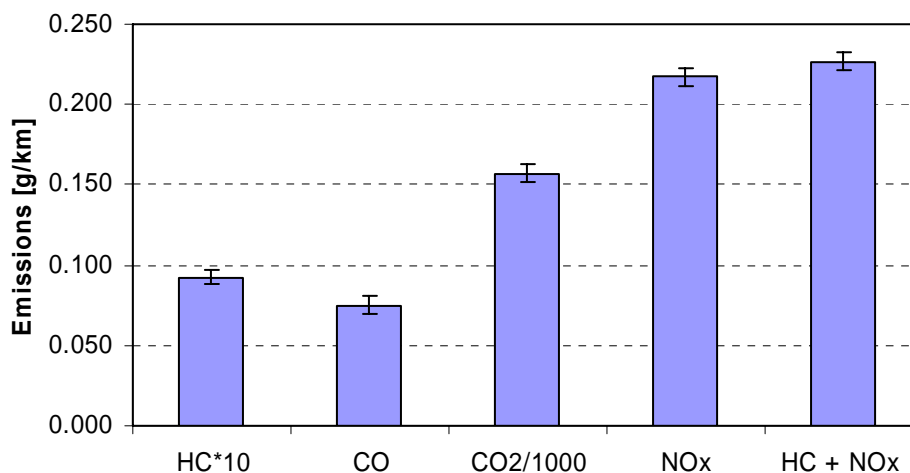


Figure 6: Gaseous emissions of valid tests. Error bars show 1 standard deviation.

Table 7: Vehicle's Regulated Emissions - Compliant With Euro 4.

Pollutant	Type Approval Emissions Data [g/km]	This study [g/km]	Euro 4 limits [g/km]
CO	0.031	0.075 (CoV 6.7%)	0.500
CO ₂	155.0	157.0 (CoV 3.5%)	-
HC + NO _x	0.182	0.227 (CoV 2.5%)	0.300
NO _x	0.166	0.217 (CoV 2.6%)	0.250
PM	0.001	0.0004 (CoV 50%)	0.025

Regeneration and -7 °C test

The gaseous and PM emissions of the vehicle for an NEDC cycle when no regeneration occurred can be seen in Figure 7 (Non-regenerating). In the same figure the emissions during a regenerating cycle are shown (Regenerating). Most emissions increase and in the case of NO_x the Euro 4 limit is exceeded by almost 100%. It must be emphasized that the regeneration was not completed in the EUDC part of the cycle and probably the emissions would be higher if a second NEDC cycle kept on without turning off the engine. However these emissions are typical for an NEDC cycle were regeneration occurs during the EUDC part of the cycle and the regeneration is not completed by the end of the cycle.

In the same figure a -7°C NEDC cycle is shown. The emissions are even higher compared to the emissions of a regenerating cycle. Poorer combustion due to fuel over-mixing, caused by extended ignition delay at cold temperatures, incomplete combustion near the cold cylinder walls during engine warm up can explain the higher emissions. Moreover, lower temperatures have as a result longer times for the catalyst to reach its "light off" temperature.

Particle number emissions

The non-volatile number emissions measured with the CPC_GOLD are shown in Figure 8. In the same figure the mass results are also shown. The mass measurements have high variability (CoV 50%), almost double than the number emissions (CoV 24%).

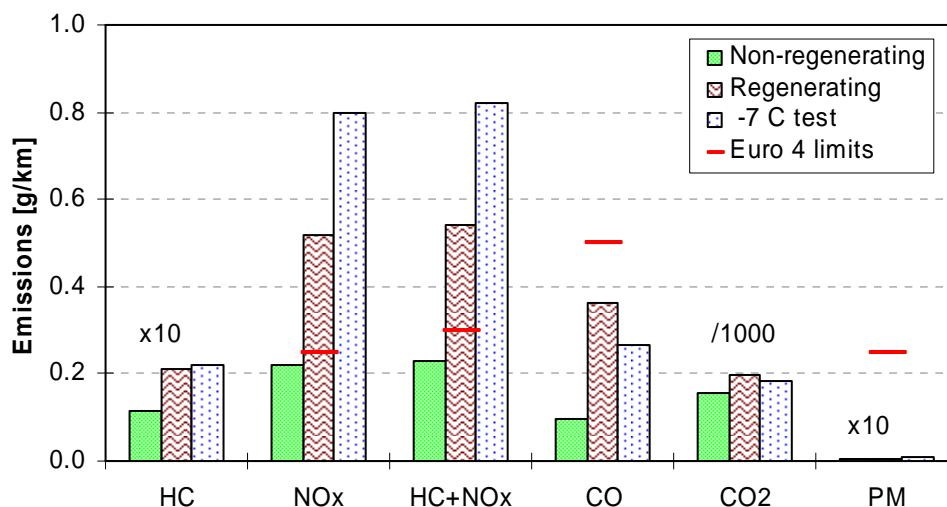


Figure 7: Gaseous and PM emissions during a non-regenerating, a regenerating and a -7°C NEDC.

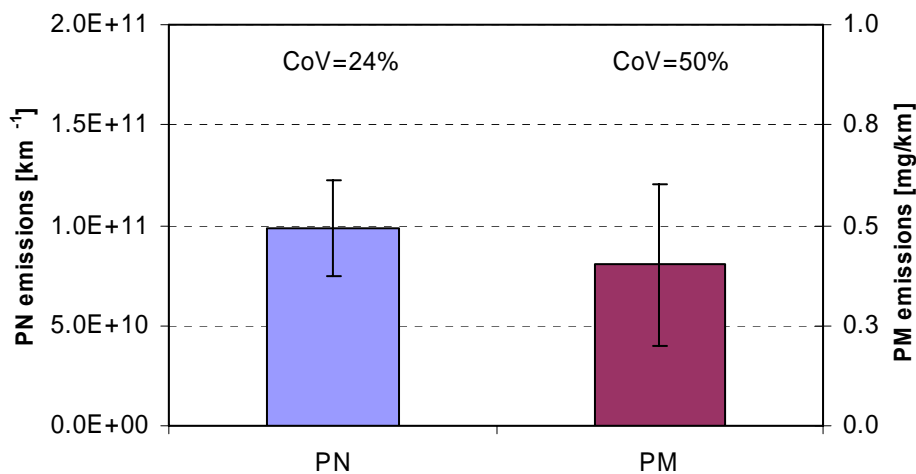


Figure 8: Particle Number (PN) and Particulate Matter (PM) emissions. Error bars show 1 standard deviation.

Real time PN emissions

Figure 9 shows the non-volatile and total PN concentration over an NEDC cycle. The concentrations are referring to the CVS and not to the vehicle tailpipe. This test is from the “NEDC Regeneration tests” period so no standard preconditioning was conducted before the measurement.

High particle concentrations are seen at the first 200 s and a noisy but at low concentrations pattern is observed at the rest of the cycle. Beginning with the part of the cycle after 200 s, it is noticed that the non-volatile particle emissions are almost zero indicating a very good efficiency of the DPF even during speed transitions. Some volatile particles are released but the concentration is low and no distinct accumulation or nucleation mode can be observed so no size distributions are shown. However, these emissions contribute less than 35% to the NEDC total particle number emissions, as the majority of the particles are emitted at the first 200 s (Figure 9).

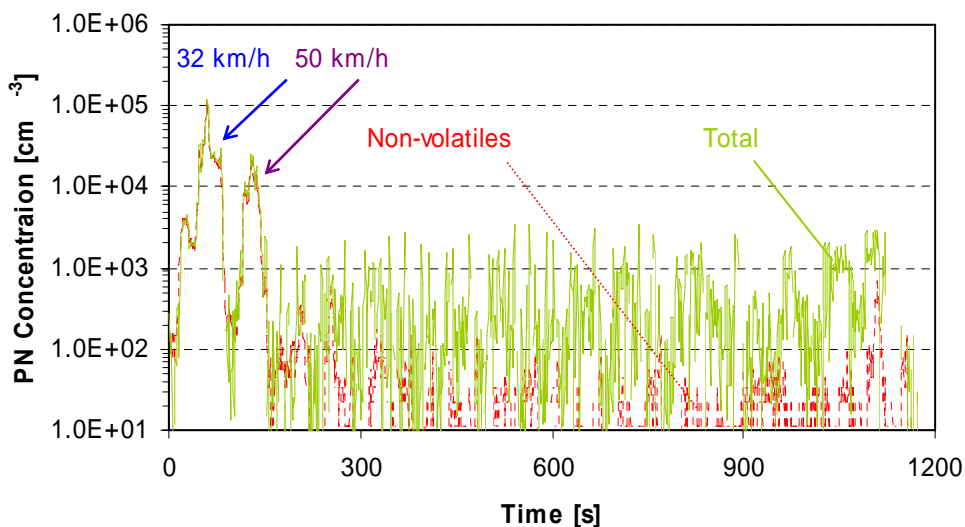


Figure 9: Non-volatile and total NEDC particle number concentration measured over an NEDC cycle. The arrows indicate the time that the size distribution of Figure 12 correspond.

Comparing EEPS and CPC and depending on the particle number concentration at the beginning of the cycle, the non-volatile particles are estimated approximately 65% of the total NEDC emissions and 97% of the total non-volatile NEDC emissions (Figure 10).

Comparing non-volatile (CPC, >22 nm) and total (EEPS, >5 nm) particle number concentrations during the first 200 s it can be concluded that the high emissions at the beginning of the cycle are mainly non-volatile particles as the two instruments show almost identical emissions (Figure 9). The same vehicle was measured in another laboratory (NTSEL), where they used a Laser Induced Incandescence (LII) instrument which measures soot particles. They also observed high non-volatile mass emissions (elemental carbon) during the first ~200s of the cycle (Figure 11). The carbon mass emissions equate to ~6 µg/km over the NEDC cycle, approximately 2% of the PM mean.

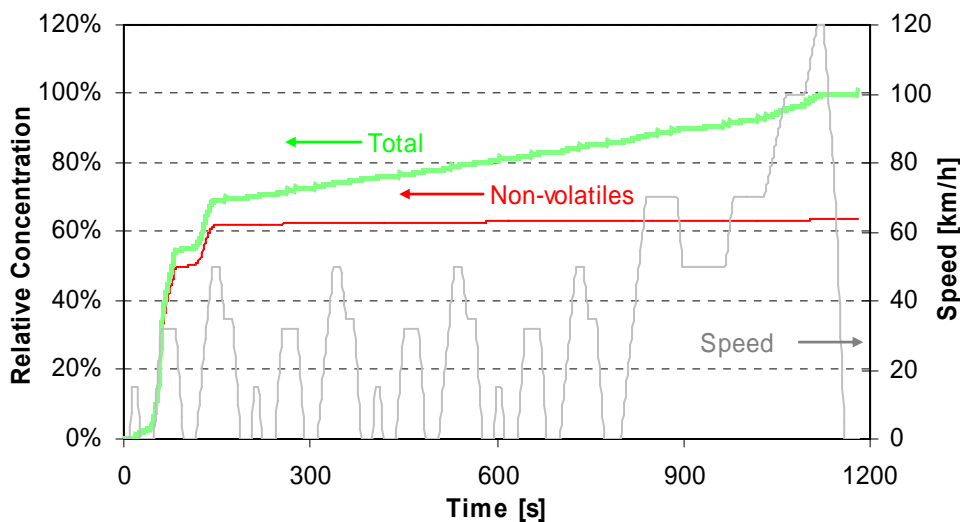


Figure 10: Relative concentration of particles over the NEDC for the data of Figure 9.

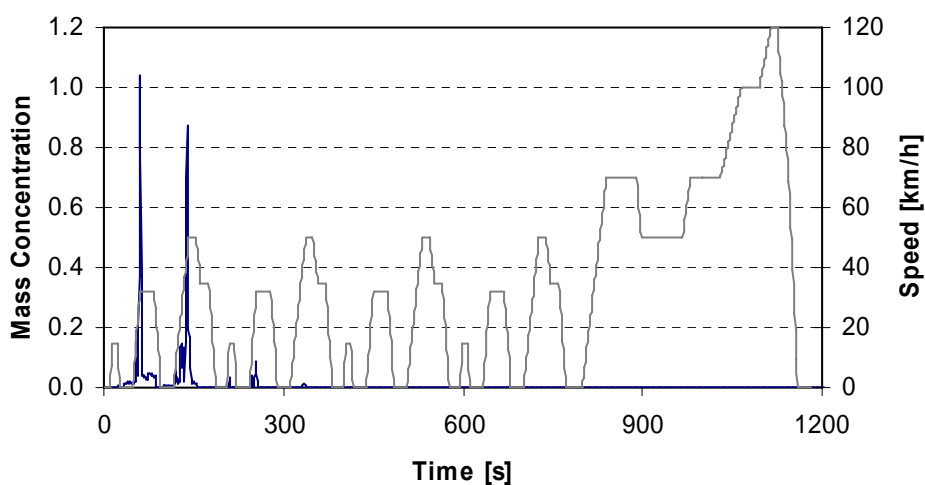


Figure 11: Real-time Emissions of Carbon from the Golden vehicle by LII (data from NTSEL).

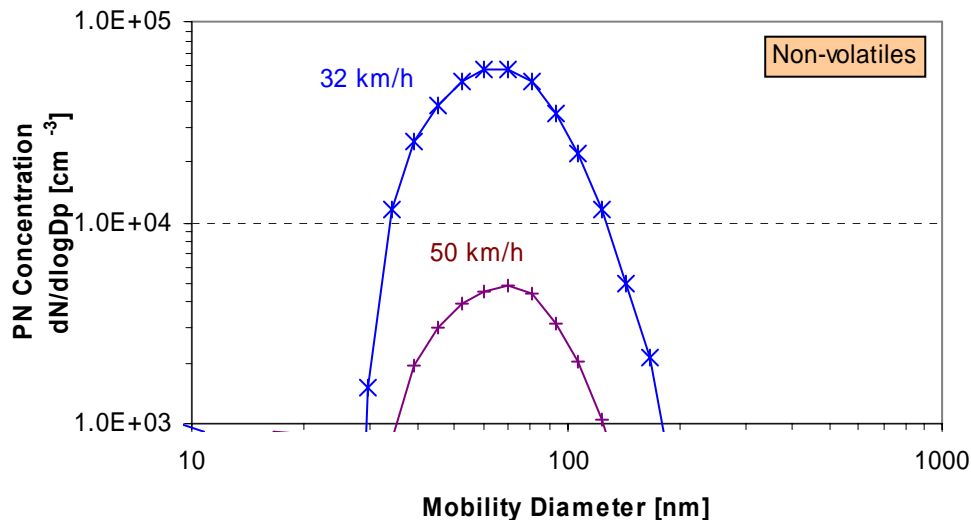


Figure 12: Cold start at 32 km/h (15 s average) size distribution measured with the EEPS (total particles) at the time indicated by an asterisk in Figure 9.

Figure 12 shows the particle number size distribution in the first 32 and 50 km/h of the NEDC cycle (averages during the 65-80 s and 145-150 s of the cycle). It is confirmed that cold start emissions consist of non-volatiles (accumulation mode soot particles) with a peak of ~70 nm. Although the magnitude of emissions changes, the size distributions are unaffected. It is also observed that particles <22 nm are negligible.

Mass comparisons

An estimate of mass concentrations can be calculated from particle size distributions measured by the EEPS. These are calculated using the particle size and number concentration by converting the size to volume and then to mass using an assumed particle density. From the EEPS manual mass concentration may be calculated from the following equation:

$$dM = dN (\pi/6) D_p^3 \rho$$

where D_p is the geometric midpoint of the particle size channel and ρ is the density. The assumption of density of 1 g/cm³ across the size range over-estimates the particulate mass contribution from the measured size distribution. Research has shown that the real density of particle agglomerates tends to decrease as mobility size increases [6]: from ~1 g/cm³ at 50 nm to ~0.4 g/cm³ at 200 nm. On this basis, the masses calculated from the EEPS data should be considered theoretical maxima, with actual masses up to 70% lower based upon the densities described above.

Figure 13 shows the mass results from different methods. Considering density of 1 g/cm³, EEPS masses comprise between 3% and 5.5% of the corresponding filter masses (when no preconditioning is conducted). This percentage increases up to 23% for tests with normal preconditioning after a regeneration where the non-volatile particle emission is high. LII, an instrument that measures soot, at NTSEL also showed that the mass of the soot of the particles emitted from the vehicle during a NEDC

cycle are only 2% of the mass calculated from the filter. These results suggest that a high amount of volatiles is collected on the filter, although an improved method is used (particles $<2.5 \mu\text{m}$, temperature $47 \pm 5^\circ\text{C}$).

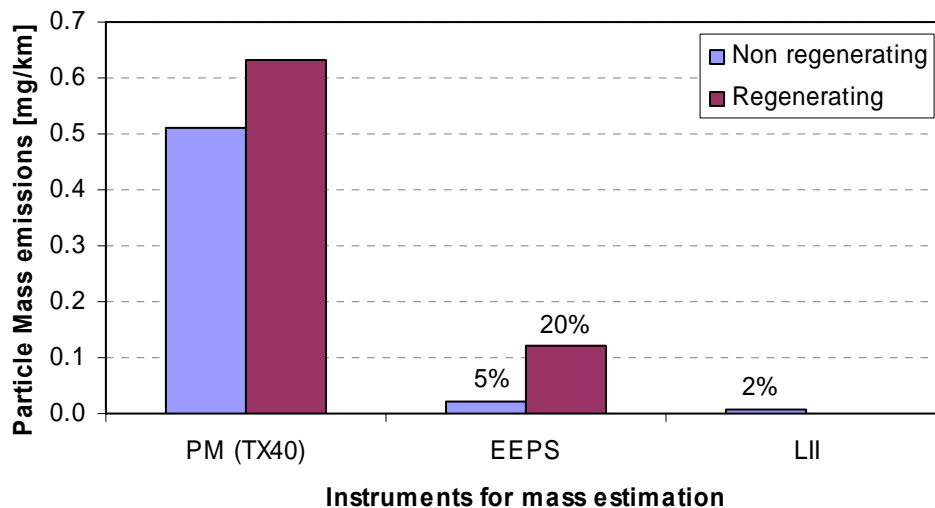


Figure 13: Comparison of mass results with different methods.

VEHICLE SOAKING AND PRECONDITIONING EFFECT

A number of experiments were conducted in order to establish any effects of different vehicle preconditioning on particle number emissions from the Golden Vehicle. The various preconditionings considered are listed in Table 8.

Table 8: Various Vehicle Preconditionings and Soakings

First Precon	Second Precon	Soak
20 min @ 120 km/h	3 x EUDC	17h
20 min @ 120 km/h	1 x EUDC	6h
None	None	None

Figure 14 compares emissions from NEDC tests following the various preconditionings. In each case, the emissions level is normalised to an NEDC result from a cold start test conducted with the full PMP preconditioning procedure (20 min @ 120 km/h + 3 x EUDC + >6h soak) that was undertaken earlier on the same day or on the previous day. From these data, it is clear that the preconditioning procedure has no effect on the particulate mass emissions from the Golden Vehicle. This is consistent with the understanding that the majority of the mass collected by the filter medium is via gas adsorption.

Experiments investigating preconditioning effects on particulate mass emissions showed no obvious effects. This was not the case with non-volatile particle number measurements. There clear effects could be seen. In general, particle numbers from NEDC cycles decreased as the severity (in terms of speed and load) of the preconditioning decreased (Figure 15). Hot start tests immediately following cold tests release virtually no non-volatile particles.

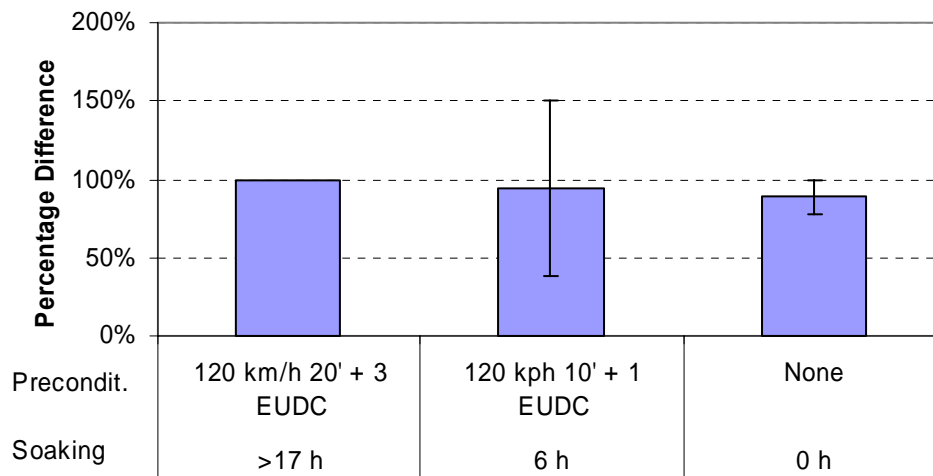


Figure 14: Effects of Vehicle Preconditioning and Soaking on Particulate Mass Emissions.

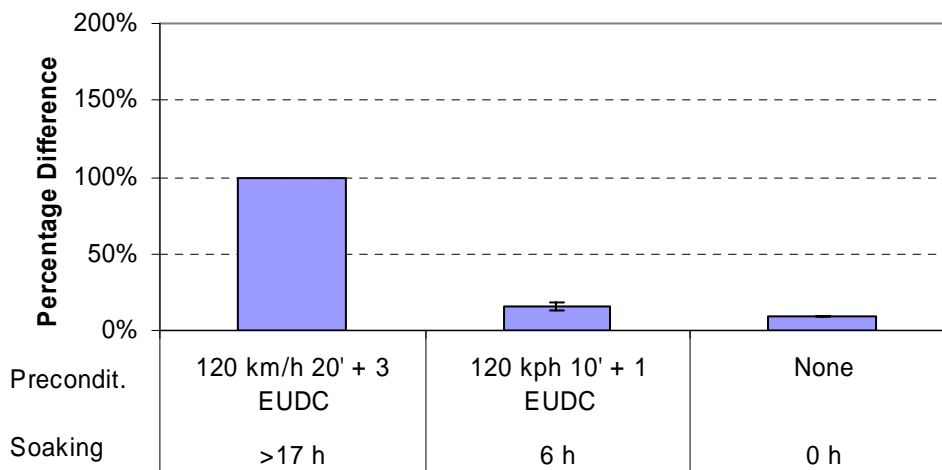


Figure 15: Effects of Vehicle Preconditioning on non-volatile Particle Number Emissions.

The differences between the cycles' particle emissions occur in the first ~3 minutes of the NEDC cycle (Figure 9) and on this basis might appear to be a cold start effect. It is hypothesised that with the Golden Vehicle and its own particular DPF, the preconditioning process loads the interstitial voids of the DPF with carbon particles during high exhaust flows and increased engine-out carbon levels. These particles settle during soak periods and are then emitted from the DPF under start-up in response to pressure changes in the particle filter (blow-out or blow-off effect). Thus elevated emissions are always seen with cold start tests relative to hot, because cold start tests have a preconditioning. There is no substantial difference between emissions from (non-regenerating) EUDC cycles irrespective of preconditioning. However, when a "cold" EUDC is run elevated particle emissions are observed (Figure 16).

It is clear that a number of these effects may combine to give the observed particle number emission level from any given test. However particle size distributions are unaffected (Figure 12). This observation can be interpreted as evidence that while the magnitude of emissions change, the chemistry of the particles – almost certainly soot – does not.

However the above mentioned are based on a limited number of tests and moreover the effect of the preconditioning and soaking cannot be completely distinguished. For this reason more measurements should be conducted.

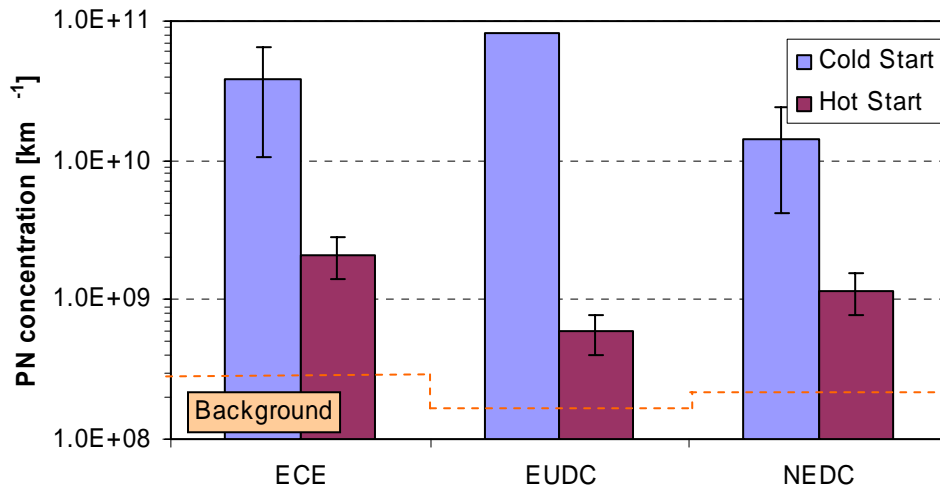


Figure 16: Comparative Cold and Hot NEDC, ECE & EUDC Particle Number Emissions (with no preconditioning).

OTHER DRIVE CYCLES

A limited number of additional drive cycles were driven on the Golden Vehicle. These included the ARTEMIS (CADC) 'real-world' urban, rural and motorway cycles [1]. As Figure 17 shows, particulate mass emissions from cold start tests tended to be higher than those from hot start tests, but most results were in the region of 1 mg/km. Hot start emissions are lower probably due to the reduced level of volatile hydrocarbons available for absorption by the filter from hot tests as the oxidation catalyst is more efficient.

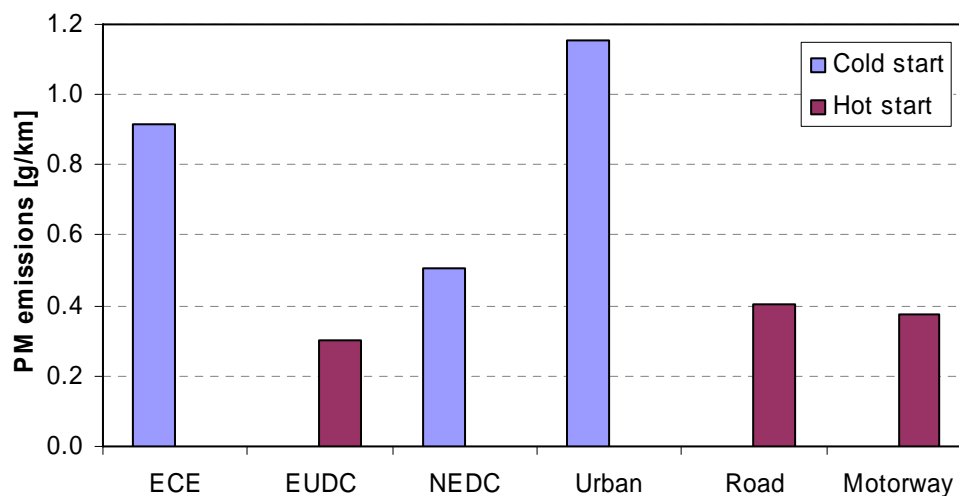


Figure 17: Particulate Mass Emissions Different Cycles.

Particle number emissions from these tests (Figure 18) showed similar trends and magnitudes to the NEDC cycle. Cold start tests (following a soak period and driven preconditioning) irrespective of cycle always gave emissions in the region of 10^{11} [km^{-1}], while hot start tests gave emissions at least a factor of 10 lower. Highest emissions were seen from the shorter cycles, with lowest emissions from the longer cycles.

From these data it is hypothesised that the particle number emissions of the vehicle are dependent primarily on the preconditioning and the filtration characteristics of the DPF. After the initial emission of carbon from the DPF – which is closely related to preconditioning- subsequent emissions are related to DPF fill (and filtration) and DPF substrate porosity. Thus emissions appear to almost independent of drive cycle: per km emissions only elevated from drive cycles that divide by small distances.

It is possible that contributions of solid non carbonaceous particles might be elevated in response to very high load and speed conditions in real-world drive cycles. However, as passive regeneration will show (Figure 33), the contribution of solid particles is expected to be small.

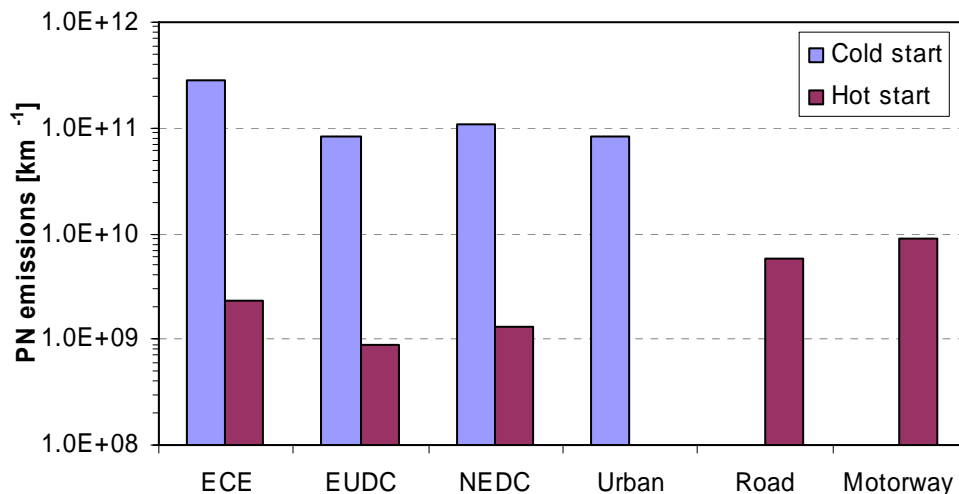


Figure 18: Particle Number Emissions – Various Emissions Cycles.

OLD AND NEW BACKGROUND

Due to some errors in the operation of the dilution air of the dilution tunnel ambient air was entering the system, leading to high particle emissions. For this reason the first measurements of the third phase were not taken into account. The background effect results have been reported [3] and can be summarized in Table 9. The background levels of mass and number present in the CVS tunnel were measured by having the anaconda blocked and measuring only the dilution air contribution for 1180s – the duration of the NEDC cycle.

Table 9: Old and new background levels.

NEDC	PM [mg/km]	GPMS [km^{-1}]
Zero		5.59×10^7
Old Background (min)	$0.585 \pm 13\%$	1.11×10^9
Old Background (min)		4.44×10^9
New Background	$0.436 \pm 22\%$	2.02×10^8

Background Particle Mass Levels and Limit of Detection

From 4 replicate background analyses the mean mass collected was 20.8 μg with a standard deviation of 4.6 μg . If sampled from the NEDC cycle, these would equate to 0.44 mg/km and 0.096 mg/km respectively. It is commonly accepted that the limit of detection (LOD) for a method can be calculated as 3 x the standard deviation of a blank measurement. If this approach is applied here, the LOD for the mass measurement method would be $\sim 13.8 \mu\text{g}$ per filter or 0.288 mg/km for the NEDC cycle.

Figure 19 compares background PM levels with the range of PM emissions observed from the Golden Vehicle during the three sets of measurements conducted. In mg/km terms, the LOD is higher than the minimum emission observed during tests by a factor of 2.5 and in addition, the mean background is higher than the mean emissions from the Golden Vehicle. For this reason the measurement of the background levels is highly recommended for each series of tests.

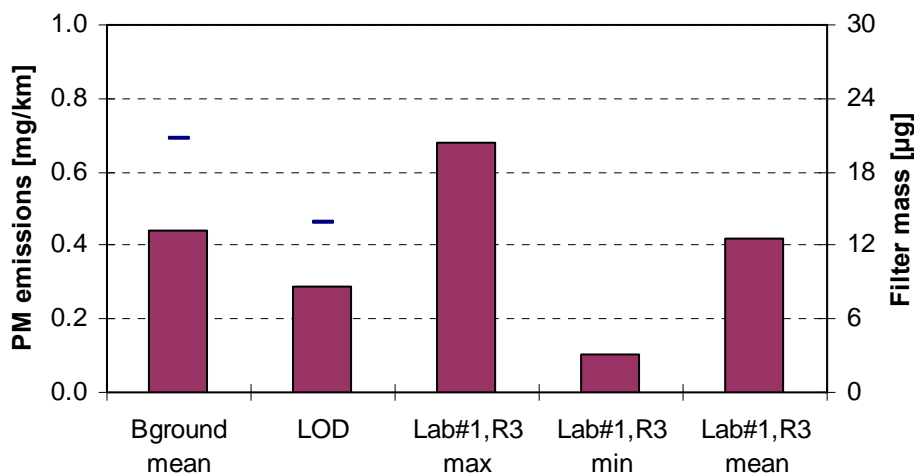


Figure 19: Comparison of Background PM and LOD with Sample PM

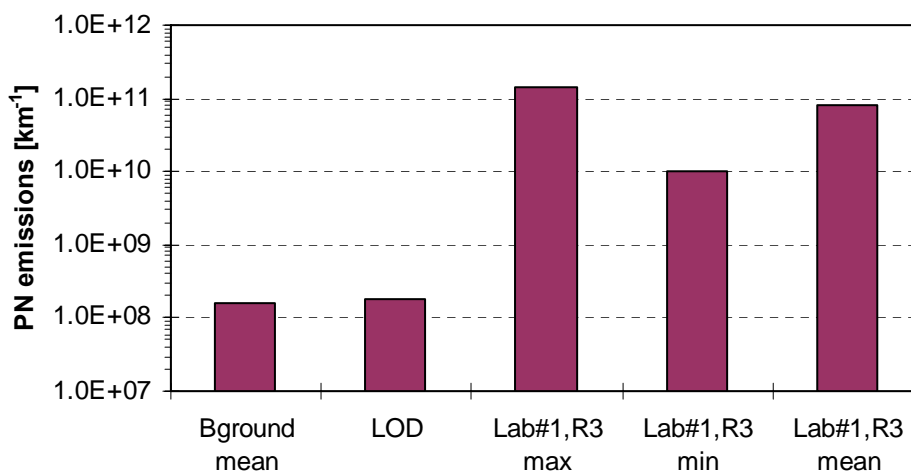


Figure 20: Comparison of Background Particle Number and LOD with JRC data (Lab#1,R3)

When the same comparative process is performed with particle number measurements, Figure 20 shows that both LOD and background levels for particle numbers are of the order $\sim 2 \times 10^8$ [km⁻¹]. Particle number LOD is 55 times lower than the lowest NEDC emissions measurement made from a cold start NEDC and 800 times lower than the highest NEDC emissions measurement made from a cold start NEDC. From these data it is clear that the number measurement method can easily discriminate between vehicle emissions and background level.

PMP AND LEGISLATED PM METHODS

The differences between the PMP mass measurement method and the legislated one are:

- PMP eliminates the use of back-up filters.
- For DPF-equipped Diesel and gasoline fuelled vehicles PMP uses a single filter for the combined urban and extra-urban phases of the NEDC, rather than separate filters.
- PMP uses a sharp cut cyclone rather than a shrouded probe.
- PMP mandates the use of TX40 glass-fibre/Teflon filters (or similar).
- PMP controls filter sampling and filter face temperature to $47 \pm 5^\circ\text{C}$ rather than merely setting an upper limit (52°C).

A limited number of experiments were undertaken after the conclusion of the validation testing to investigate the influences of these factors.

Single vs. Multiple and Backup Filter Effects

Figure 21 shows the mass emissions levels from the Golden Vehicle recorded using a single filter for the entire NEDC (1 Filter), a single filter with a back-up (F +Backup) and using two filters without back-ups (ECE+EUDC). Error bars show 1-standard deviation. Experiments were undertaken twice in the same day. The afternoon tests have lower emissions due to the “lower” preconditioning used (see paragraph “Vehicle soaking and preconditioning effect”).

A comparison between the 1 Filter and F + Backup results shows that the backup filter collects up to $\sim 25\%$ (or 0.1 mg/km) of the primary filter mass level and that the back-up filter mass is more variable than the primary filter mass. The most substantial effect though, is the increase in apparent mass emissions between the 1 filter result and the ECE+EUDC result. This increase, up to $\sim 30\%$ in these experiments (or 0.15 mg/km), is probably due to the doubling of any volatile collection artifact related to the filter medium used.

These results are specific to Diesel vehicles equipped with highly efficient wallflow DPFs and may not represent effects from higher porosity substrates which may leak carbon. However from the most efficient DPF types, combining the effects of eliminating backup filters and moving from 2 filters to a single filter per NEDC cycle suggests that measured PM levels will be reduced by 30% (or 0.2 mg/km) relative to the current filter method.

Figure 22 shows the PN emission results. PN emissions are not affected by the PM measurements and show the stability of the vehicle in the specific measurements.

Cyclone and Filter Heating Effects

Limited testing has been conducted using the PMP mass method with and without the cyclone and sampling system heater employed. As Figure 23 shows, it appears that there is no effect of the cyclone and heating.

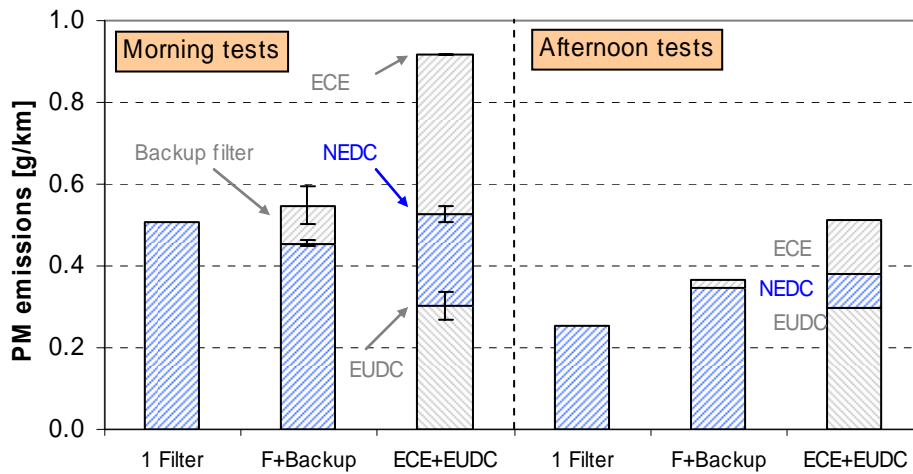


Figure 21: Effect on PM emissions of different filter configurations.

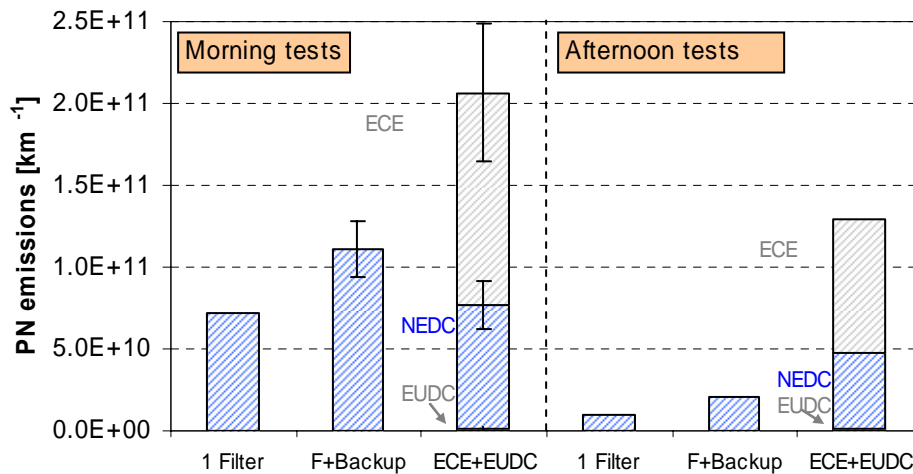


Figure 22: PN emissions stability during the filter mass measurements of Figure 21.

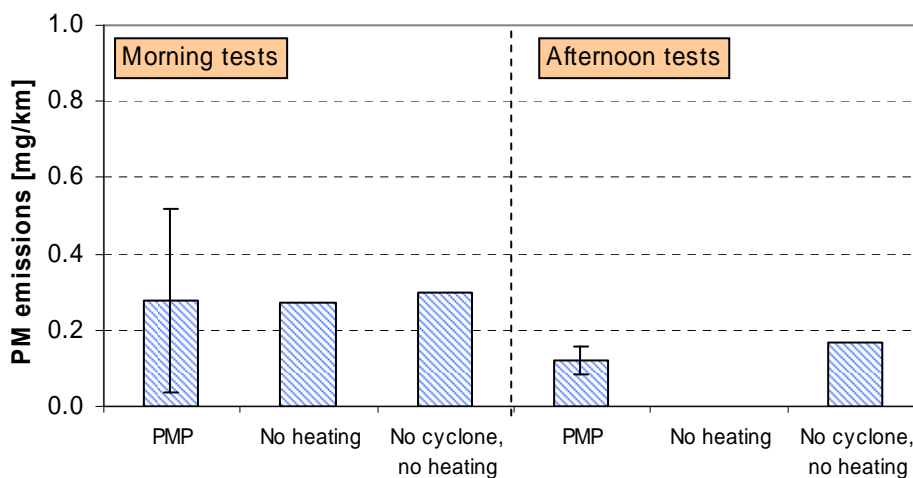


Figure 23: Effects of cyclone and system heating on mass emissions.

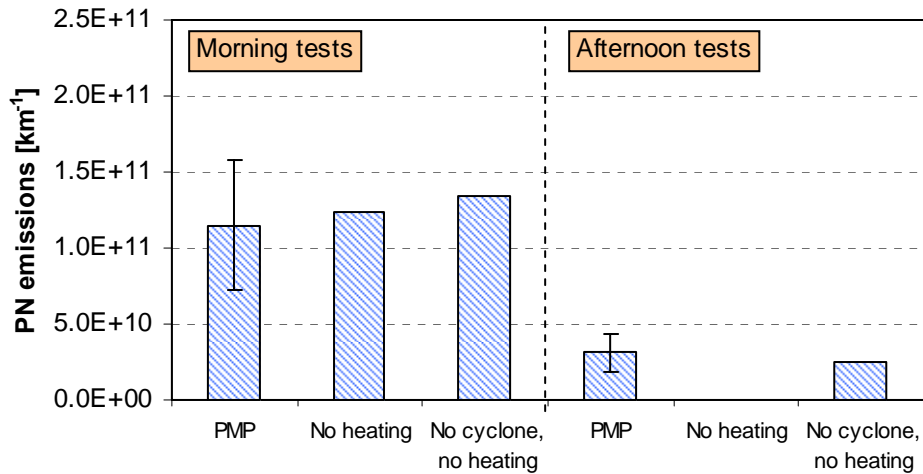


Figure 24: PN emissions stability during the filter mass measurements of Figure 23.

Filter Media Effects

Comparative measurements using TX40 and Teflo filters (Figure 25) on the Golden Vehicle were done. It was not possible to perform both measurement sets simultaneously, so comparisons shown are from the average of several tests with each method. With the exception of the filter medium, all other sampling parameters were constant and Teflo filters were treated with an antistatic neutralizer prior to weighing in order to dispel any static charge. This is particularly important following testing.

No significant differences were determined between methods, though a background level similar to the filter loading was found. This background level is thought to contribute to the masses found on both Teflo and TX40 filters and is almost certainly comprised of volatiles. This can be seen in Figure 26, which shows that while the mass background was equivalent to the mass collected from the emissions cycle, the non-volatile particle number background (where volatiles are eliminated by the VPR) is between 100 and 1000 times lower than the measured particle number emissions.

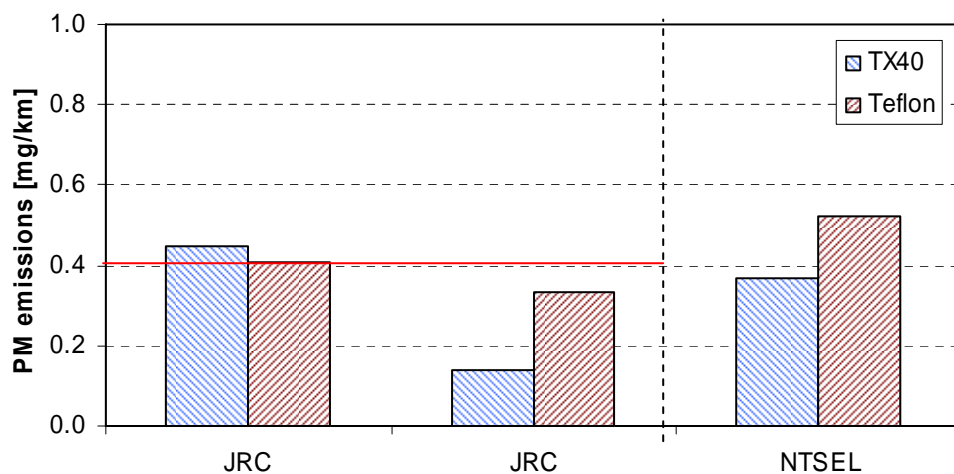


Figure 25: Comparison of mass emissions with 2 different filter media.

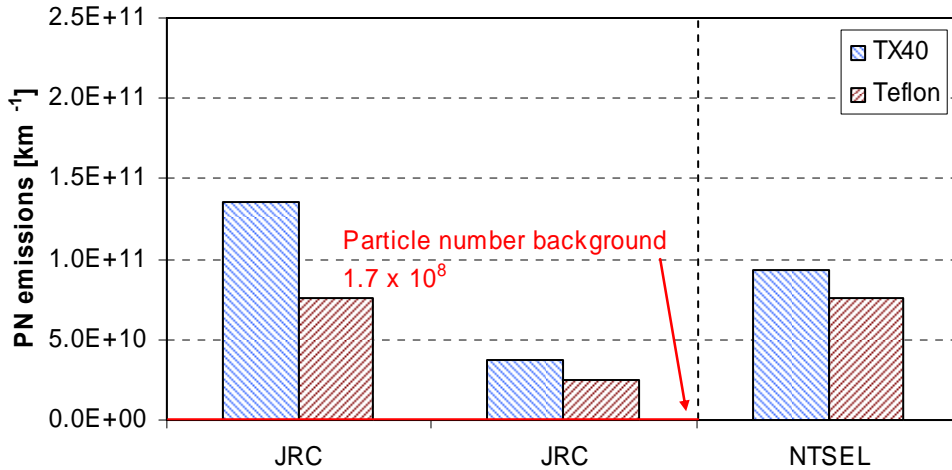


Figure 26: Particle Number emissions and background during filter media tests of Figure 25.

BEFORE-AFTER REGENERATION

Figure 27 shows the non-volatile and total particle number concentration over NEDCs just before and almost immediately after a regeneration event. Before these tests standard preconditioning was conducted. As it can be seen non-volatile particle number emissions at the beginning of the cycle (before 300 s) are higher after the regeneration event compared to before the regeneration event. This can be attributed to the lower filtering efficiency of the DPF after the regeneration, where no soot cake has been accumulated in the DPF channels. Total NEDC particle number emissions are almost 3 times higher after the regeneration compared to before the regeneration.

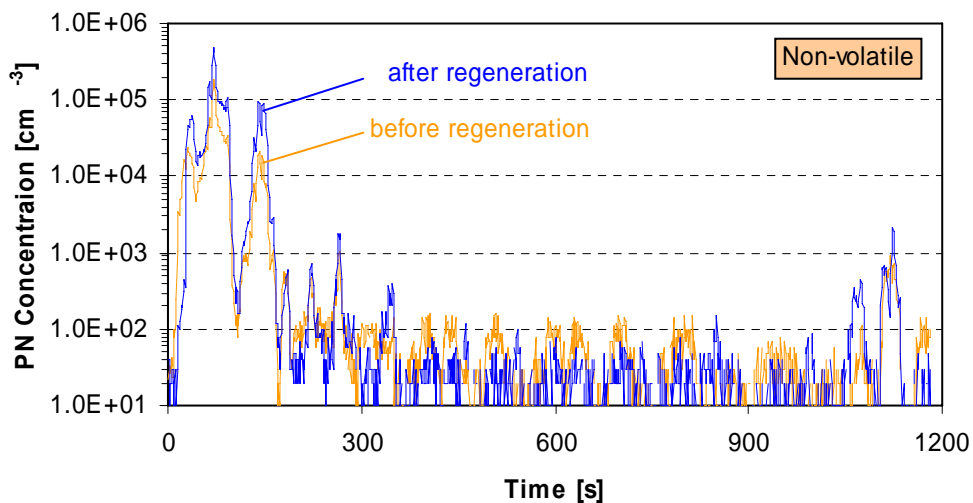


Figure 27: Non-volatile particle number concentration over NEDC before and after a regeneration event (with standard preconditioning).

REGENERATION EMISSIONS

Figure 28 shows total and non-volatile particle concentrations over a cycle in which regeneration occurred. The cold start emissions over the ECE were discussed previously. The regeneration takes place in the EUDC part and will be discussed in this section.

Non-volatile particle emissions during the EUDC increase compared to a non regenerating cycle (see e.g. Figure 9 EUDC part of the cycle) but remain much lower compared to the cold start emissions at the beginning of the cycle. This increase can be attributed to the net loss of soot from the DPF during the regeneration and the resulting reduced filtering efficiency of the DPF.

However, total particle number concentration over the EUDC part of the cycle increases by many order of magnitudes and overreaches even the cold start emissions at the beginning of the cycle. These particles may initiate from sulfate nuclei with condensed hydrocarbons. Probable sources of sulfates are the sulfur that is adsorbed on the soot, the sulfur that is trapped in the DPF and the sulfur in the aftertreatment devices. Moreover sulfur from the fuel that is injected into the catalyst to heat the DPF may play an important role.

NEDCs were run without any preconditioning in between, as mentioned in the test protocol section. Regeneration was observed over 8 NEDCs. It should be stressed that the sequence of stop-start regenerations that were observed is not representative of the regulatory approach to assessing particulate mass emissions - that is conducted so that a regeneration occurs and completes during one or two continuous NEDC cycles, the first being cold. However, the set of partial regenerations seen might be a good indicator of 'round-town' operation, where incomplete regenerations could be common.

Figure 29 shows 11 NEDC tests where regeneration occurred in tests #3-10. Only the EUDC part of the cycle is shown for the particle number emissions (Figure 29a) as regeneration initiates in this part. Moreover this way the cold start (blow out) effect discussed previously was excluded, as the conditioning of the vehicle in these tests was different. It can be seen that during all regeneration events the EUDC total particle number emissions are very high: in the order of 10^{13} km^{-1} . If stored sulfur was the main source of NM a decreasing NM concentration from test to test would be seen. So probably the sulfur in the fuel that is injected for the regeneration seems to be the main sulfuric acid contributor. The high temperatures during the regeneration increase the SO_2 to SO_3 conversion rate [7].

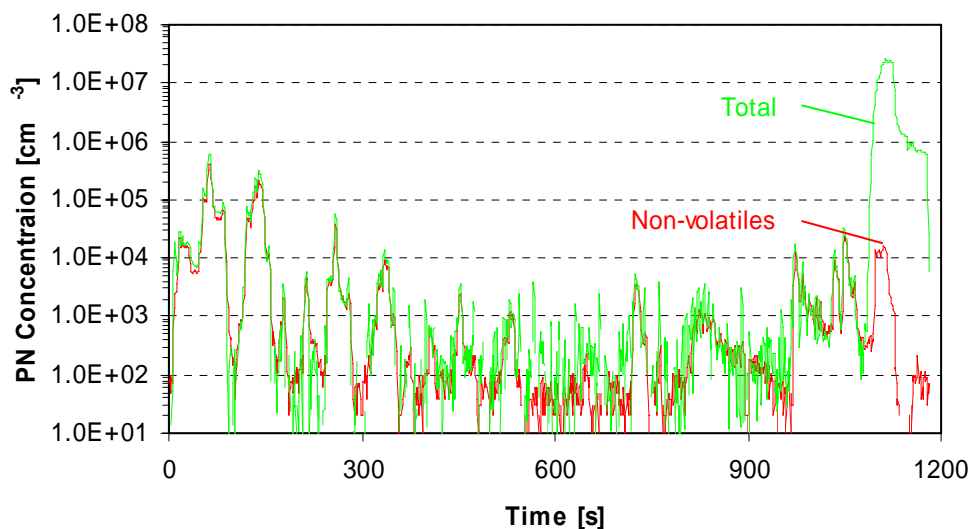


Figure 28: Total and non-volatile particle emissions during a regenerating cycle.

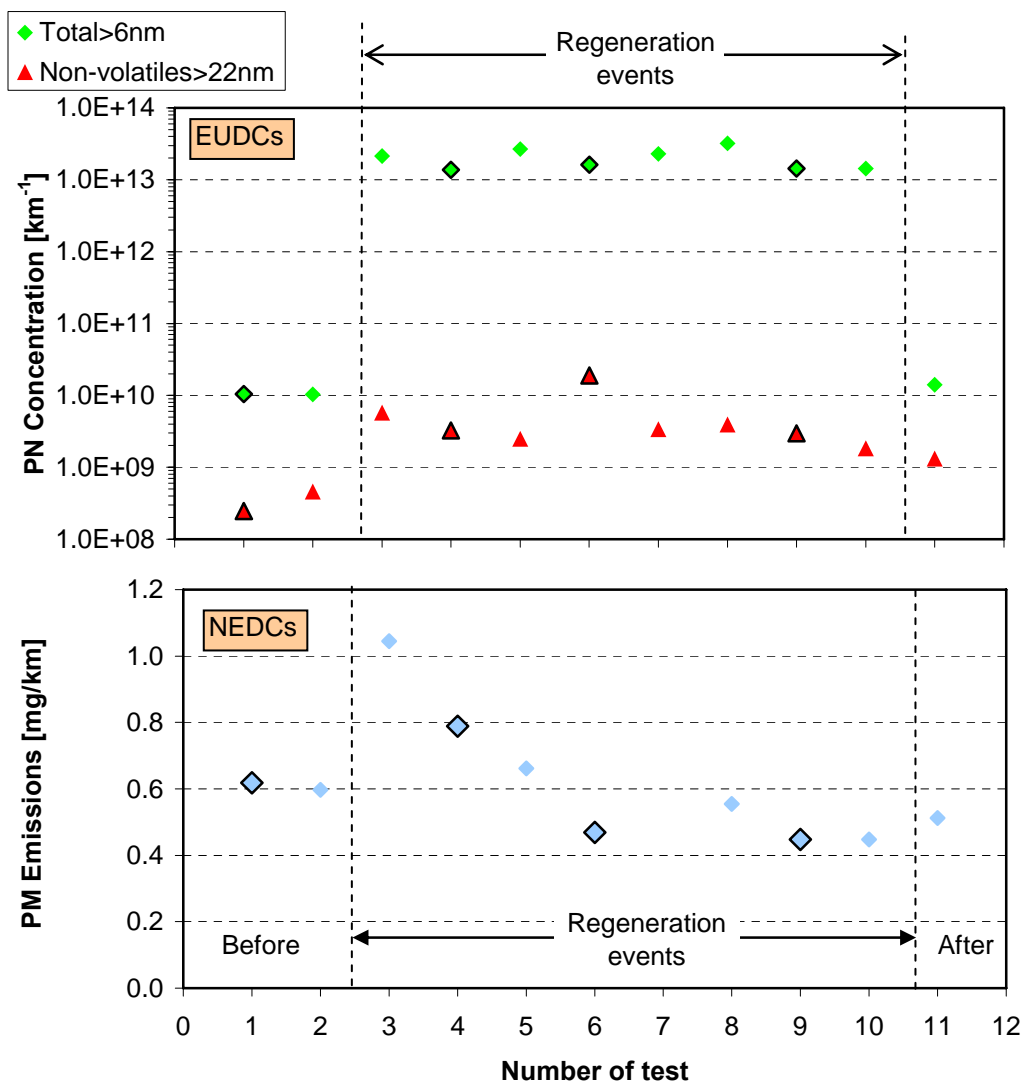


Figure 29: a) Particle number emissions over EUDCs. b) PM emissions over NEDCs before, during and after regeneration events. Bigger points with black foreground line correspond to cold start NEDCs. Smaller points are hot start NEDCs.

Figure 29a also confirms that non-volatile particle number emissions during and after the regeneration event are higher compared to those before the regeneration event. As it was discussed in the paragraph “Before-after regeneration”, the cleaning of the DPF during the regeneration results in a decreased filtration efficiency and consequently more particles are emitted during speed transitions.

PM emissions over the NEDC (Figure 29b) show high emissions at the first regeneration test that decrease afterwards to reach a lower PM level than before the regenerations. The lower emissions after the regeneration event, which are in contrast with the lower filtering efficiency of DPFs, can be explained from the deposition of volatile material on the walls of the exhaust tailpipe downstream of the DPF [8, 9] and the dilution tunnel. During regeneration, because of the higher temperatures, some volatile material

is released and higher emissions are measured. In subsequent cycles volatiles are stored again and consequently lower PM emissions are being measured after a regeneration event.

Size distributions

To better investigate the high emissions during the regenerations for the 8 EUDC cycles (#3-10) size distributions are reported in Figure 30. Three kinds of size distributions were observed depending on the time that the NM appeared (Figure 30):

- NM appearing during the acceleration between 70 and 100 km/h.
- NM appearing during the end of 100 km/h.
- NM appearing during 70 km/h.

In the first case (Figure 30a) NM appears at the acceleration between 70 and 100 km/h. The NM increases as the speed increases and maximizes at 100 km/h (NM size at 35 nm). These particles (>22 nm) are not non-volatiles as the CPC concentration remained at low levels during the EUDC. As discussed previously sulfur might be one precursor. However it is believed that purged volatile materials stored in the exhaust system that combine with unburned fuel and lubricant HCs form larger droplets (35 nm) under initial regeneration conditions. The interesting point is that a few seconds later, during the acceleration between 100 and 120 km/h the already formed NM concentration decreases (see size distribution 115 km/h) but a new NM peak appears possibly due to increased SO₂ to SO₃ formation. This peak maximizes at 120 km/h (NM size at 10 nm). During the deceleration it sharply decreases as the temperature is not high enough to convert the SO₂ to SO₃. This kind of regeneration appeared only at the first regeneration event (cycle #3 as coded in Figure 29).

In the second case (Figure 30b) NM appears at the end of the 100 km/h constant speed part of the EUDC. However, as the speed increased to 120 km/h (and the exhaust gas temperature also) the NM also increases due to the increased SO₂ release and the higher SO₂ to SO₃ conversion. This SO₃ with the available HCs form a NM with high concentration and size of 12.5 nm as soon as they are cooled and diluted in the CVS. As the first regeneration purged most volatile material, available HCs for condensation in this case are mainly those which were stored during the ECE part of the cycle. In this case solid particles <22 nm cannot be excluded from the NM although their contribution should be small. These could probably be ash or fuel additive based metallic oxides. During the deceleration phase NM decreases as described previously. This kind of regeneration appeared in cycles #4, 5, 6, 7, 8 (as coded in Figure 29).

Finally, at the last cycles (#9, #10 from Figure 29) NM appeared at the phase of the cycle where speed was constant at 70 km/h (Figure 30c). At this speed the temperature is much lower, so lower SO₂ conversion rates are expected. In addition, the stored sulfate and HCs are expected to be lower due to the high amounts that were released in the previous regenerations. Thus the NM concentration in this case is very low and is decreasing even when the speed increases. However, at 120 km/h there is an indication of NM at diameters <6 nm that cannot be measured by the EEPS because of its measurement limits.

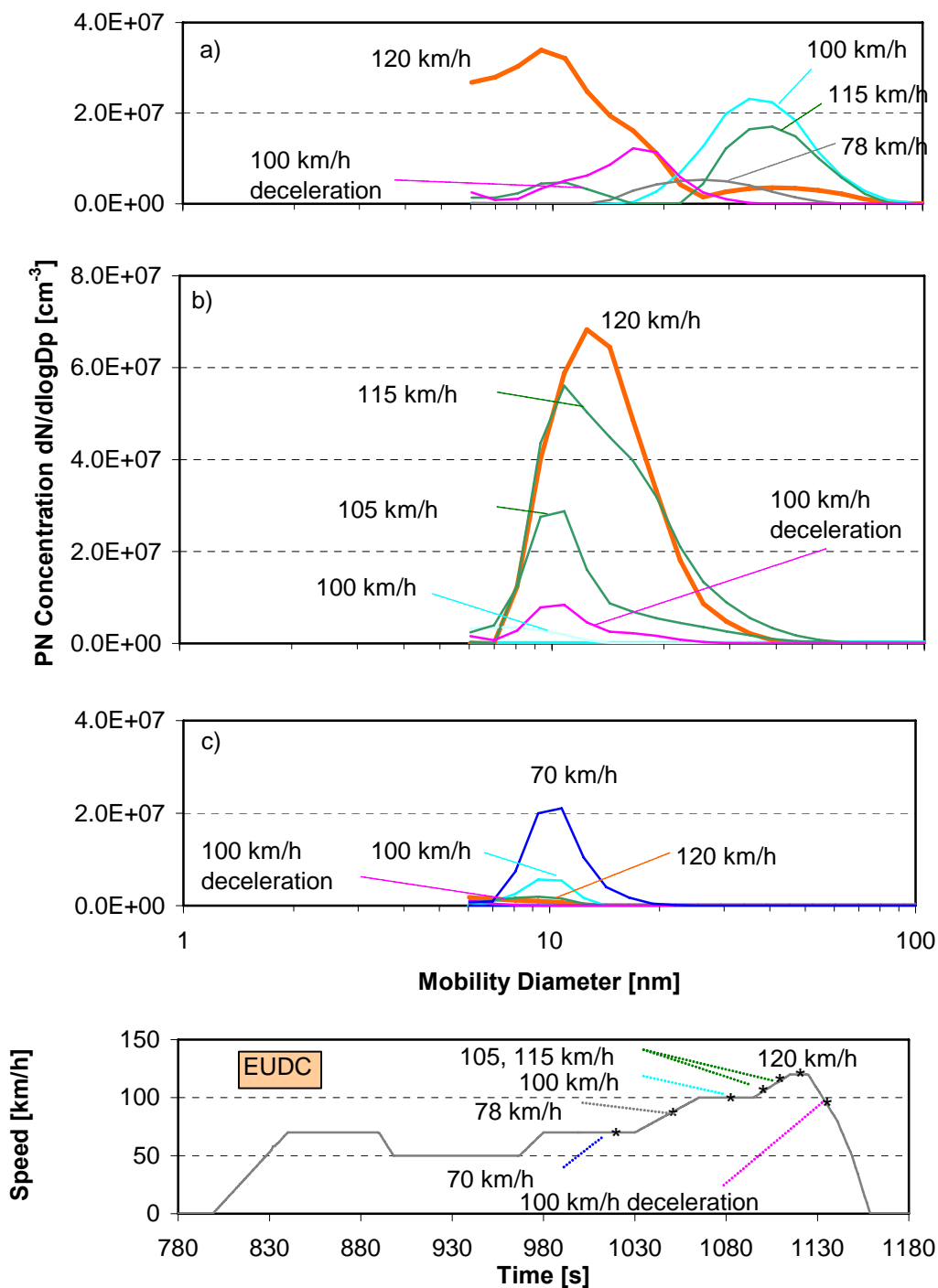


Figure 30: Particle number size distributions during regeneration events where NM appeared a) during the acceleration of 70 to 100 km/h b) during 100 km/h c) during 70 km/h. Each size distribution corresponds to 1 second of measurements. The exact times of the measurements are shown at the bottom of the figure.

Regeneration during steady state tests

During a 120 km/h steady state (Figure 31) emissions levels from CPC_REF (Semi+Non-volatile) and CPC_GOLD (Non-volatile) are highly similar: no semi-volatile particles penetrate the initial hot dilution stage at this operating condition.

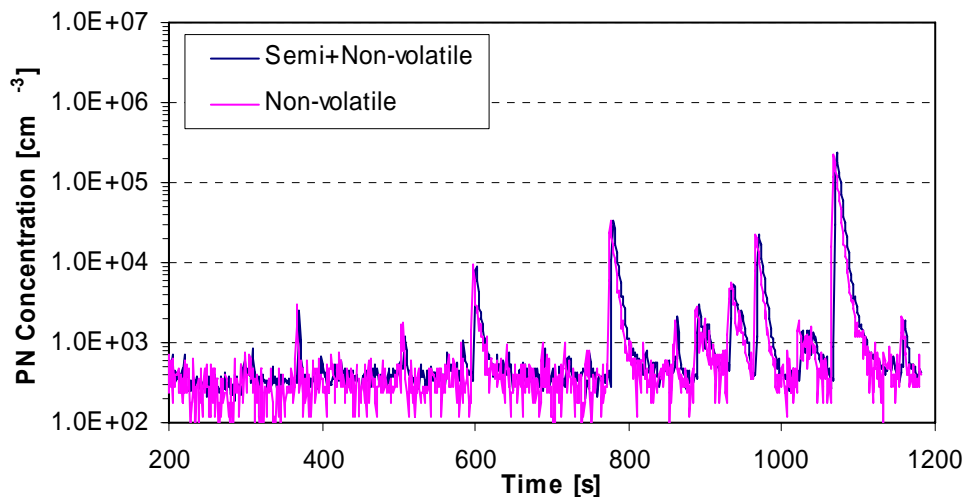


Figure 31: Particle number emissions by CPCs during 120 km/h cruise.

However, when an active regeneration is observed during a 120 km/h steady state (Figure 32), many volatile particles are observed. This type of regeneration throttles the engine, shuts down EGR and injects fuel very late in the engine cycle (post-injection). This results in elevated exhaust temperatures and a substantial level of fuel surviving to combust across the oxidation catalyst but limits the level of oxygen. Soot on the DPF, which incorporates cerium, combusts emitting CO₂. Ultimately this led to exhaust temperatures ~100°C higher than from a non-regenerating 120 km/h steady state. Of the particles that penetrate the primary diluter, at least 99% are eliminated by the evaporation tube and can be considered semi-volatiles. A rapid increase in non-volatile particle emissions occurs at the end of the regeneration (NO_x emissions return to normal levels). In Figure 32 this occurred at ~670s. However particle number emissions remained elevated for more than 5 min. Non-volatile particles emitted are believed to be comprised of both elemental carbon from particulate which is incompletely oxidised and very low volatility hydrocarbons. The low volatility HCs may be lubricant derived species that are either stored on the DPF through adsorption with carbon and evaporate during regeneration, or are materials that slip through the DPF when filtration efficiency and exhaust temperatures are low and condense in the exhaust system. These are then released in response to high thermal temperatures in the exhaust [9].

A passive DPF regeneration – where exhaust temperatures and oxygen levels are sufficiently high to enable cerium doped carbon to combust without any additional thermal assistance from engine changes – was observed during a steady state cruise at 140 km/h. Semi-volatile particle emissions (Figure 33) measured by CPC_REF increased by ~475x and non-volatiles (measured by CPC_GOLD) by ~2.5x in response to the regeneration, in each case by substantially less than from the active regeneration at 120 km/h (Figure 32). During the passive regeneration soot oxidation may be more efficient than from

the active regeneration due to a surplus of oxygen, and exhaust temperatures will be lower: the former leading to reduced carbon particle emissions and the latter to reduced volatile particle emissions.

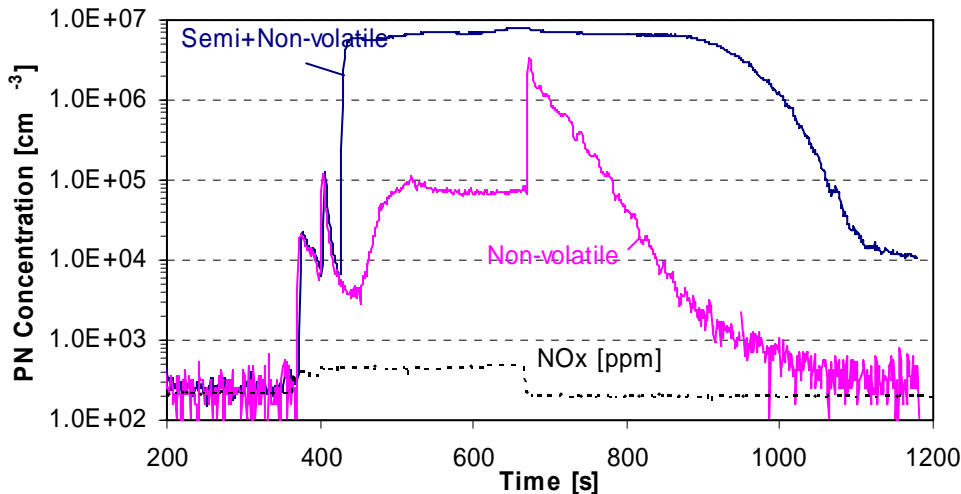


Figure 32: Particle number emissions by CPCs during 120 km/h active regeneration.

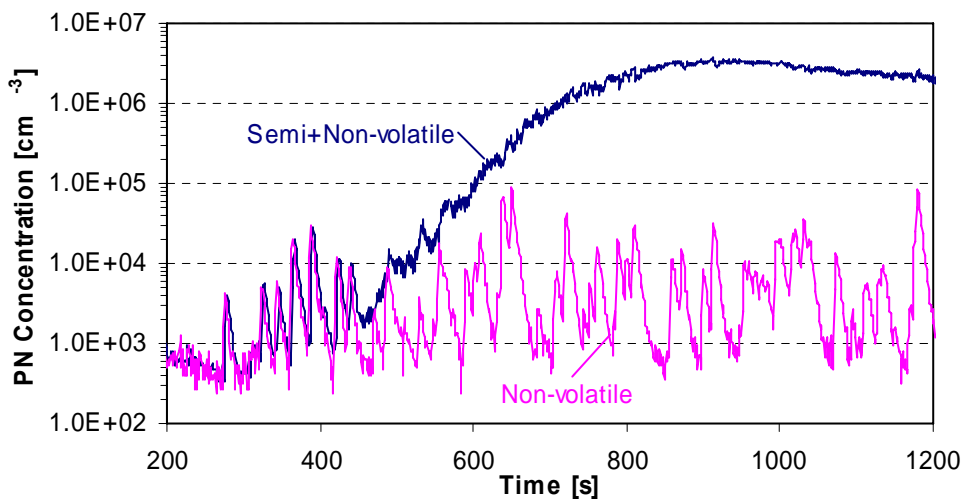


Figure 33: Particle emissions during passive regeneration at 140 km/h.

A summary of the emissions during active and passive regeneration can be seen in Figure 34. Non-volatile particle emissions (measured by CPC_GOLD) rose by a factor of ~60: from 2.56×10^9 to 1.52×10^{11} [km^{-1}] between the non-regenerating and regenerating steady states, but semi-volatile particles (measured upstream of the evaporation tube by CPC_REF) showed a more than ~2000 times increase (2.78×10^9 to 5.60×10^{12} [km^{-1}]).

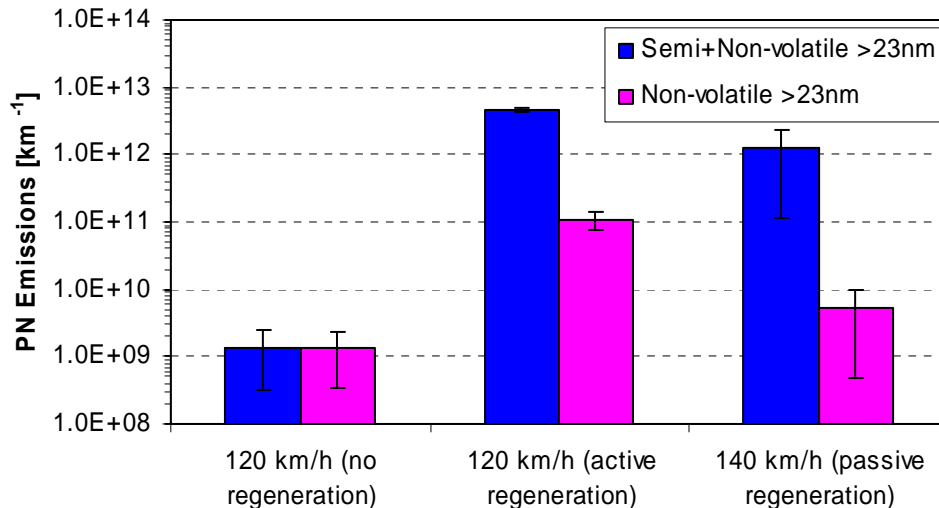


Figure 34: Particle emissions during steady state regenerations. Error bars show min and max measurement of 2 tests.

DPF STABILIZATION

The difference in particle emissions before and after a regeneration event which was discussed in Figure 27 can lead to repeatability problems, so there was an effort to identify the necessary stabilization distances. Figure 35 shows the NEDC emissions after two different regeneration events over the mileage driven. For all these cycles the soaking was >17 h and the preconditioning was the standard. Squares indicate one set of measurements after a regeneration event and triangles another set of NEDCs.

Non-volatile particle number emissions are high after the regeneration event and seem to stabilize after 300 km at a lower level. If the point at ~700 km is excluded from the analysis, particle emissions for the first 300 km are $1.4 \times 10^{11} (\pm 32\%) \text{ km}^{-1}$, while after 300 km are $9.8 \times 10^{10} (\pm 15\%) \text{ km}^{-1}$. Although the difference is not statistically significant there is an indication of decreased variability and lower emission levels after 300 km. This is believed to be related to the progressive filling of the DPF and increase in filtration efficiency as mileage is accumulated.

PM emissions on the other hand are lower after the regeneration event and need higher distance to stabilize. PM emissions for the first 350 km are $0.35 \pm 22\% \text{ mg/km}$, while after 350 km (excluding the two points with emissions <0.2 mg/km) are $0.5 \pm 16\% \text{ mg/km}$. If the two points are taken into account, PM emissions are $0.44 \pm 38\% \text{ mg/km}$.

The same behavior of PM and number emissions was also noticed during the NEDC regeneration tests (see Figure 29). Although the particle number behavior can be explained theoretically, the PM behavior can only be explained by increased adsorption after the regeneration event (as discussed in Figure 29).

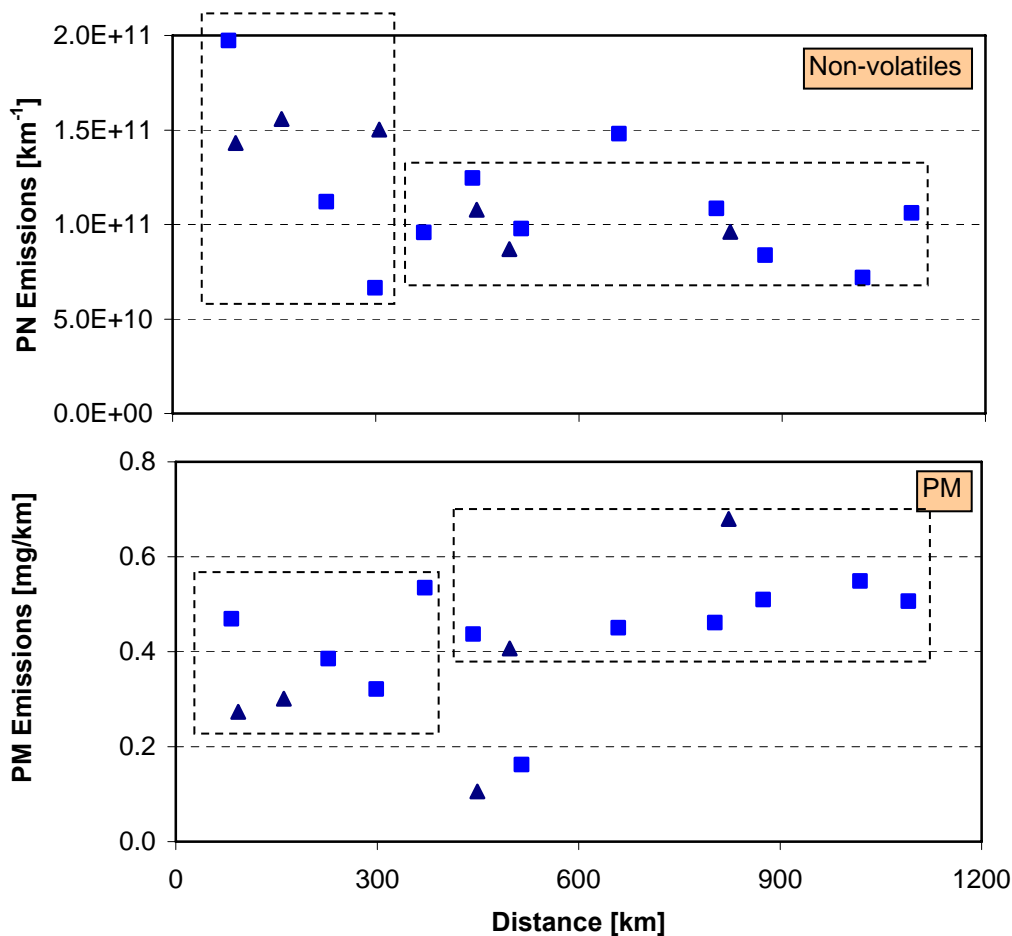


Figure 35: Stabilization distance after regeneration events.

COMPARISON OF THE THREE PHASES

JRC measured at the beginning (JRC#1) [10], in the middle (JRC#2) [11] and at the end of the light-duty inter-laboratory correlation exercise (JRC#3). In this section the emissions of the vehicle of these three phases will be compared.

The stability of the vehicle can be checked from the gaseous emissions. Figure 36, Figure 37, Figure 38, Figure 39 show the CO₂, CO, NO_x and HC emissions. CO₂ of the third phase was lower compared to the first phase (Figure 36). CO of the third phase was higher compared to the first two phases (Figure 37). It is considered likely that test work conducted at JRC#2 which involved active and passive regenerations of the DPF, may have led to a small change in the vehicle operation and/or catalyst function and thus affected emissions. These active and passive regenerations were representative of real-world driving and could similarly influence emission levels during in-service operation. Nevertheless, this effect did not affect considerably the rest pollutants. NO_x and HC emissions were at the same levels for all three phases (Figure 38 and Figure 39).

Figure 40 shows the PM emissions and Figure 41 the PN emissions. Mass emissions of the third phase were at the same level as with the first phases, but the scatter was higher, probably due to the changes of the dilution air system and the longer duration of the measurements. Number emissions of the third phase were between the two phases with a similar scatter.

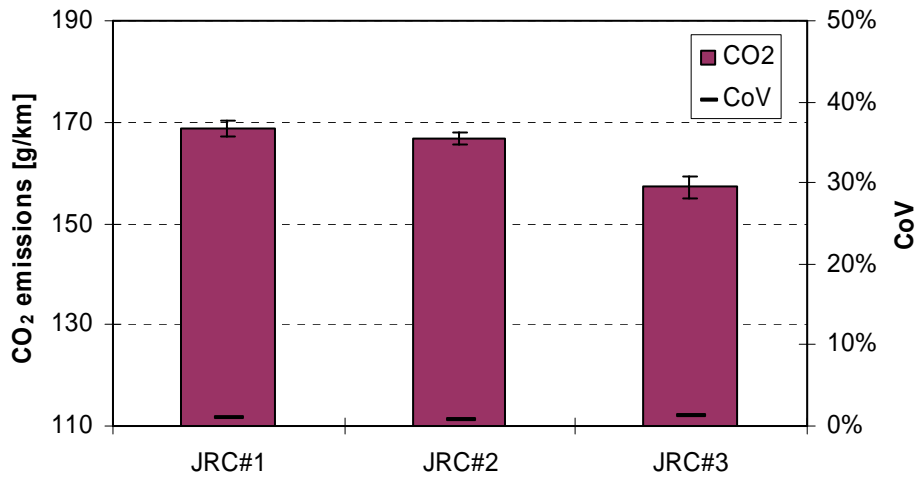


Figure 36: CO₂ emissions at the three JRC phases.

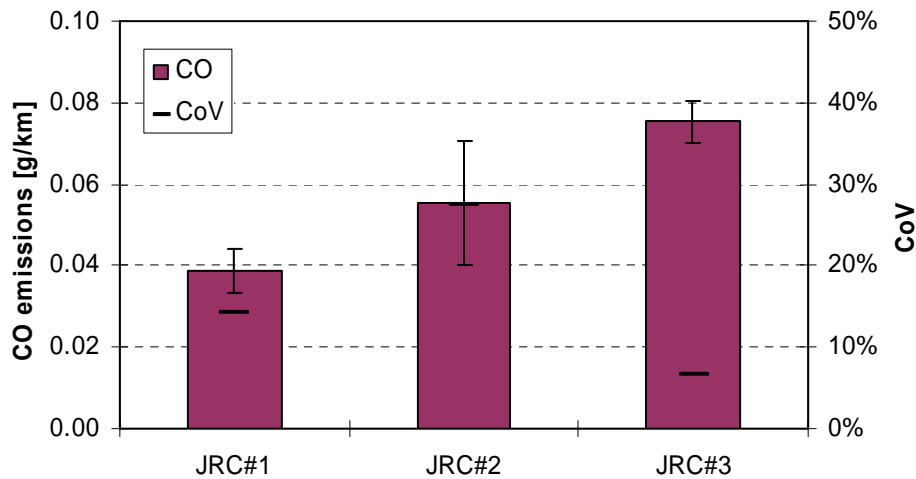


Figure 37: CO emissions at the three JRC phases.

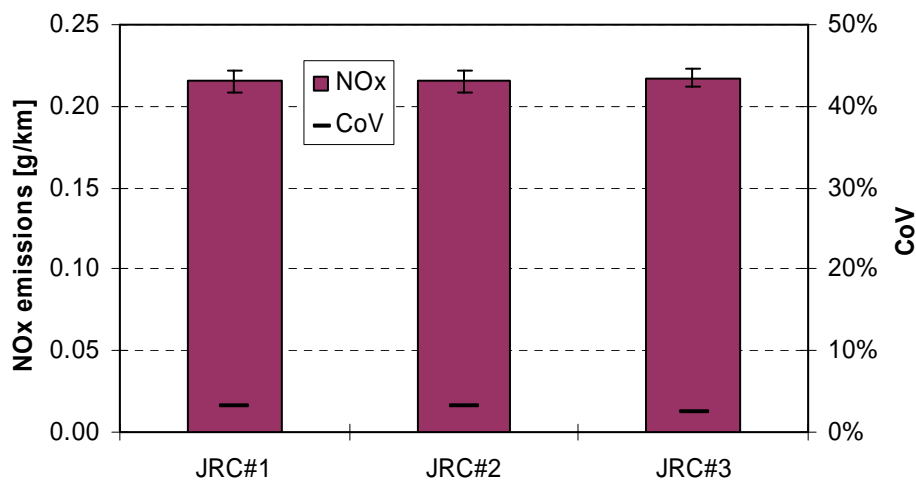


Figure 38: NO_x emissions at the three JRC phases.

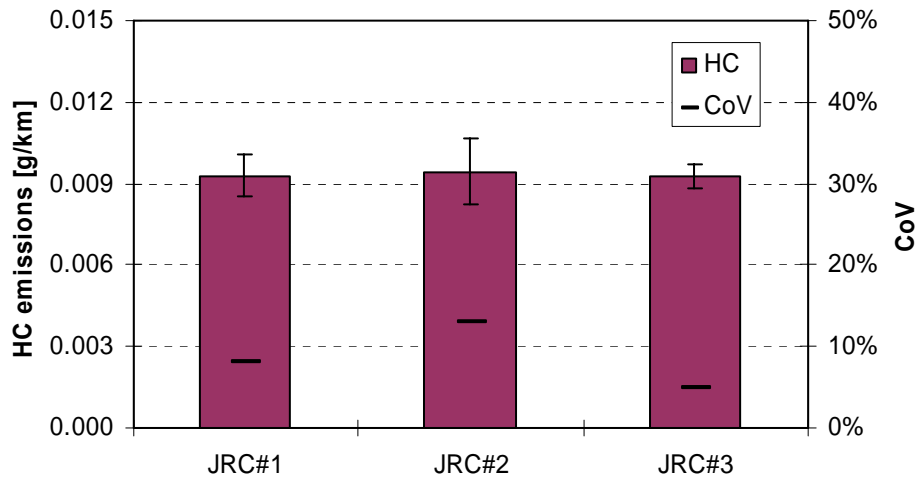


Figure 39: HC emissions at the three JRC phases.

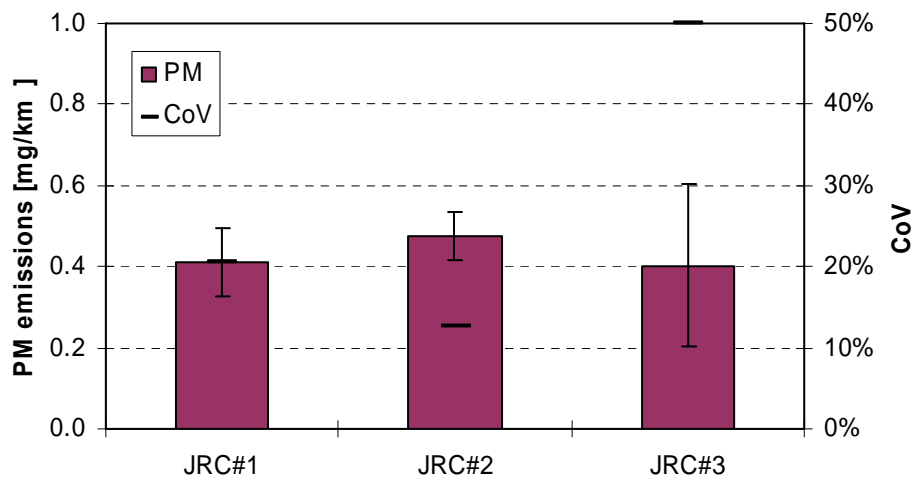


Figure 40: PM emissions at the three JRC phases.

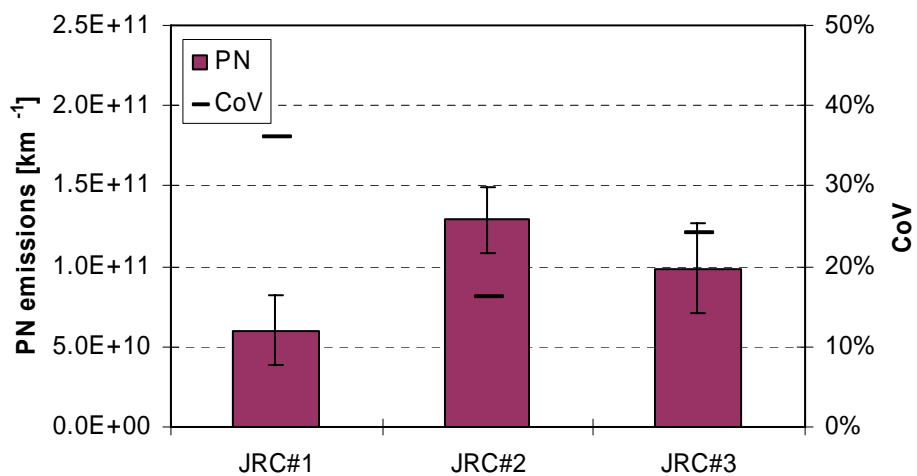


Figure 41: Particle number emissions at the three JRC phases.

4. DISCUSSION & CONCLUSIONS

This phase of measurements studied the emissions of a light-duty Diesel vehicle equipped with a Diesel Particulate Filter (DPF) and employing a fuel-borne catalyst (FBC) to aid regeneration. Low sulfur fuel (8 ppm) and lubricant (<0.2%) were used according to the PMP protocol. The main conclusions of the tests in JRC follow; the results of the project can be found in [12].

PHASE #3 RESULTS

The mass emissions of the vehicle were 0.4 mg/km with a CoV of 50%. The number emissions were approximately $\sim 1 \times 10^{11}$ with a CoV of 24%. The gaseous emissions of the vehicle were below the Euro 4 limits. Emissions during regeneration and a low temperature start (-7 °C) test showed increased gaseous emissions (especially NO_x).

EXTRA MASS TESTS

The backup filter collected up to ~25% (or 0.1 mg/km) of the primary filter mass level and that the back-up filter mass was more variable than the primary filter mass. Increase, up to ~30% in these experiments (or 0.15 mg/km), was observed by using separate filters at the ECE and EUDC parts of the cycle probably due to the doubling of any volatile collection artifact related to the filter medium used.

No effect of the heating and the cyclone was observed.

No difference in the PM emission was observed using Teflo or TX40 filters.

PARTICLE NUMBER EMISSIONS

Figure 42 summarizes NEDC non-volatile and total particle number emissions before, during and after a regeneration event. The contribution of the ECE and EUDC part of the cycle is shown with a horizontal line. The contribution is calculated simply by dividing ECE or EUDC emissions [km⁻¹] with the sum of ECE and EUDC emissions [km⁻¹]. The conclusions are:

Cold Start emissions

The majority of non-volatile particle number emissions of this vehicle (>95%) are emitted at the first 200-300 s of the cycle. This can be attributed to a “blow-out” of non-volatile particles during the first seconds of the cycle due to changes in the flow, pressure and temperature. Preconditioning and the fill state of the DPF also play an important role. The more vigorous a preconditioning phase, the higher the non-volatile particle number emissions since particles are forced into the walls of the DPF and released during the next cold start test.

During the rest of the cycle non-volatile particle number emissions are at background levels because the DPF has reached an equilibrium state and has a high filtration efficiency. For this reason emissions appear to almost independent of drive cycle: per km emissions only elevated from drive cycles that divide by small distances.

Not many volatile particles are observed during the cycle and they contribute less than 35% of the total NEDC emissions.

Before-After regeneration

Non-volatile and total particle number emissions at the ECE part of the cycle during and immediately after a regeneration event are higher than before the regeneration. This can be attributed to the better filtration efficiency of the loaded DPF due to the formed soot cake. The emissions of the EUDC part are also higher but they remain at low levels compared to the ECE cold start emissions.

During regeneration

As it can be seen in Figure 42, total NEDC particle number emissions during a regeneration event increase up to 2 orders of magnitude.

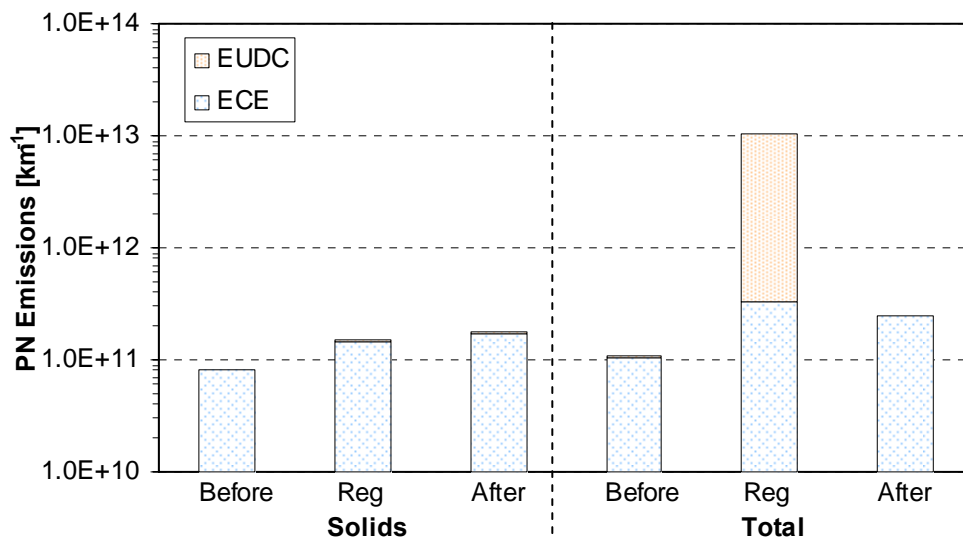


Figure 42: Particle number emissions before, during and after a regeneration. The contribution of ECE and EUDC emissions is given with a horizontal line which is calculated by simply dividing ECE or EUDC emissions [in km⁻¹] with the sum of ECE and EUDC emissions [in km⁻¹].

The non-volatile particle number emissions increase more than 50% compared to the pre-regeneration emissions because the DPF has been cleaned. However they are at the same level as the post-regeneration emission levels.

NM size distributions during regeneration events show a dependence on the stored material (in the DPF and the rest exhaust system) and the speed (which affects the exhaust gas temperature). In the first regeneration event a NM with peak at high diameters (~35 nm) can be observed due to the purge of stored volatile material that combines with unburnt fuel and lubricant. In subsequent speed changes or regeneration events the peak is smaller (~12 nm) due to the smaller amount of released volatiles. In the final regeneration events the NM peak (and concentration) is very low due to the minimal sulfur and HCs release.

Stabilization times

In order to avoid the emission level differences before and after a regeneration event, based on the experiments of this study, stabilization distances of approximately 300-400 km are recommended. This means that at least 35% of the regeneration interval mileage should be accumulated after regeneration before a vehicle is tested in order to ensure repeatability for repeatable measurements.

PM suitability

Although, after a regeneration event particle numbers increase compared to the pre-regeneration event, PM shows the opposite trend. This might be explained by increased adsorption and storage after the regeneration event, even though an improved mass measurement method (filter temperature of 47°C



($\pm 5^{\circ}\text{C}$) and one filter for the whole NEDC cycle) was used. This effect and the low sensitivity of the method with these low vehicle emission levels raises concerns about the suitability of the PM method for the future vehicle technologies.

COMPARISON OF THREE PHASES

No long term change of the behavior of the vehicle was noticed by comparing the gaseous emissions of the three phases. Mass and number emissions of the three phases were also at the same levels.

References



- [1] de Haan P.; Keller M. (2001). Real-world driving cycles for emission measurements: ARTEMIS and Swiss cycles. INFRAS report for BUWAL, Switzerland, 17 March 2001
- [2] Andersson, J; Clarke, D. (2004). UN-GRPE PMP Phase 3: Inter-laboratory correlation exercise: Framework and laboratory guide. <http://www.unece.org/trans/doc/2005/wp29grpe/PMP-2005-14-01e.pdf>
- [3] Giechaskiel, B. (2006). Background levels and effect on particle emissions. Internal unit report
- [4] Kittelson, D.B.; Watts, W.F.; Johnson, J.P.; Rowntree, C.; Payne, M.; Goodier, S.; Warrens, C.; Preston, H.; Zink, U.; Ortiz, M.; Goersmann, C.; Twigg, M.V.; Walker, A.P.; Caldow R. (2006). On-road evaluation of two Diesel exhaust aftertreatment devices. *J. Aerosol Sci.*, 37, 1140 – 1151
- [5] Maricq, M.M.; Chase, R.E.; Podsiadlik, D.H.; Vogt R. (1999). Vehicle exhaust particle size distributions: A comparison of tailpipe and dilution tunnel measurements. SAE Technology Paper 1999-01-1461
- [6] Park, K., Cao, F.; Kittelson, D.; McMurry, P. (2003). Relationship between particle mass and mobility for diesel exhaust particles. *Environ. Sci. Technol.*, 37, 577-583
- [7] Giechaskiel, B.; Ntziachristos, L.; Samaras, Z.; Casati, R.; Volker, S.; Rainer, V. (2007). Effect of speed and speed transition on the formation of nucleation mode particles from a light duty diesel vehicle. SAE Technology Paper 2007-01-1110.
- [8] Giechaskiel, B.; Ntziachristos, L.; Samaras, Z.; Casati, R.; Scheer, V.; Vogt, R. (2005). Formation Potential of Vehicle Exhaust Nucleation Mode Particles On-Road and in the Laboratory, *Atmospheric Environment*, 39, 3191-3198
- [9] Andersson, J.; Jemma, C., Bosteels, D.; Searles, R. (2002). Particle emissions from a EU 3 heavy-duty diesel engine with catalyst-based diesel particle filter and selective catalytic reduction system: Size, number, mass & chemistry. 11th Aachen Colloquium on Vehicle & Engine Technology, 2002
- [10] Muñoz-Bueno, R.; Dilara, P.; Manfredi, U.; Colombo, R. (2005). PMP Inter-laboratory Correlation Exercise: Report on PART 1: JRC Tests in Nov.'04. EUR 21858 EN
- [11] Muñoz-Bueno, R.; Dilara, P.; Manfredi, U.; Colombo, R. (2006). PMP Inter-laboratory Correlation Exercise: Report on PART 2: JRC Tests in May'05. EUR 22202 EN
- [12] Andersson, J.; Giechaskiel, B.; Muñoz-Bueno, R.; Sandbach, E.; Dilara, P. (2007). PMP LD Inter-laboratory Correlation Exercise: Final Report. EUR 22775 EN

DEFINITIONS, ACRONYMS, ABBREVIATIONS

CADC:	Common ARTEMIS Driving Cycles
CoV:	Coefficient of Variance
CPC:	Condensation particle Counter
CVS:	Constant Volume Sampler
DPF:	Diesel Particulate Filter
ECE:	Urban Driving Cycle
EEPS:	Engine Exhaust Particle Sizer
EGR:	Engine Gas Recirculation
ET:	Evaporation Tube
EUDC:	Extra Urban Driving Cycle
FAP:	Filtre à Particules
FBC:	Fuel Borne Catalyst
FID:	Flame Ionization Detector
GOLD:	Golden
HC:	Hydrocarbon
JRC:	Joint Research Centre
NEDC:	New European Driving Cycle
NM:	Nucleation Mode
PAO:	Polyalphaolefin
PDR:	Primary Dilution Ratio
PM:	Particulate Matter
PN:	Particle Number
PMP:	Particle Measurement Programme
REF:	Reference
SDR:	Secondary Dilution Ratio
VELA:	Vehicles Emissions Laboratory

ANNEXES

Annex A. Test fuel specifications for the Golden Vehicle

 Direction Additifs et Carburants Spéciaux Chemin du canal - BP 22 - 69360 Solaize France Tél: +33 4 78 02 60 64 - Fax: +33 4 78 02 60 91				
APPELLATION : GAZOLE TYPE CEC RF 06-03		Référence analyse : 8180		
GAZOLE INDUSTRIE	N° de lot : B7274081	Date : 03/09/2004		
CERTIFICAT DE CONFORMITE <input checked="" type="checkbox"/>		BULLETIN D'ANALYSES <input type="checkbox"/>		
GAZOLE	SPECIFICATIONS	UNITE	RESULTATS	METHODES
DONNEES PHYSIQUES				
Masse Volumique 15 °C	833 à 837	kg/m3	835	ASTM D 4052
Viscosité à 40°C	2.3 à 3.3	mm2/s	2,7	ASTM D 445
DISTILLATION				
PI		°C	185	ASTM D 93
5 % Vol		°C	201	ASTM D 93
10 % Vol		°C	208	ASTM D 93
20 % Vol		°C	219	ASTM D 93
30 % Vol		°C	233	ASTM D 93
40 % Vol		°C	261	ASTM D 93
50 % Vol	246 mini	°C	274	ASTM D 93
60 % Vol		°C	283	ASTM D 93
70 % Vol		°C	308	ASTM D 93
80 % Vol		°C	320	ASTM D 93
90 % Vol		°C	333	ASTM D 93
95 % Vol	345 à 360	°C	348	ASTM D 93
PF	370 maxi	°C	368	ASTM D 93
E 250 °C		%Vol	38,8	ASTM D 93
E 350 °C		%Vol	98	ASTM D 93
E 370 °C		%Vol	98,5	ASTM D 93
INDICE DE CETANE				
Cétane calculé		Index	63,5	ASTM D 4737
Cétane mesuré	62 à 64	Index	63	ISO 5165-98
Point Eclair	66 mini	°C	75	EN 22719
COMPOSITION				
Aromatiques Totaux		%Mass	21,8	IP 391
Poly-Aromatiques	3,0 à 6,0	%Mass	4,4	IP 391
TENUE AU FROID				
Point de trouble		°C	-9	ASTM D2500
TLF	-5 maxi	°C	-18	EN 115, NF M 07042
COMBUSTION				
Pouvoir Calorifique Intérieur (G)		MJ/kg	43,355	ASTM D 4053
%C, %H, %O		%Mass	87,4/11,4/0,6	GC / Calculated
DONNEES COMPLEMENTAIRES				
Stabilité à l'Oxydation	25 maxi	g/m3	10	ISO 12205
Corrosion Cuivre 3H, 50°C	C1	merit	1a	ASTM D 130
Soufre	10 maxi	mg/kg	8	ISO 4260 / ISO 8754
Carbone Conradson sur résidu 10% Vol	0.2 maxi	%m/m	0	ISO 10370
Teneur en cendres	0.01 maxi	%m/m	0,01	ISO 6245
Indice d'acide	0.02 maxi	mg KOH/g	0	ASTM D 974
Teneur en sédiments		mg/kg	2	ASTM D 2276
Teneur en esters méthyliques d'acides gras	néant	%Mass	0	
Teneur en eau	200 maxi	mg/kg	65	EN ISO 12937
Pouvoir Lubrifiant à 60°C	400 maxi	µm	380	ISO/DIS 12155
Observation :				
VALIDATION LABO le 24/09/2004 par Mehdi KELLE 		Document confidentiel. Diffusion extérieure soumise à l'accord de RM/SPEIACS L'interprétation des résultats des mesures relève de la norme NF EN ISO 4259 Fiche de données de sécurité : 50030000 DE / EN / ES / FR / IT		
Date specs : 26/06/2003 Rév: 0				

24/09/2004

Annex B. Third phase of measurements in JRC.

Mileage	Date	Test id	PN [# /km]	PM	HC	HC+NOx	CO	NOx	CO2	COMMENTS
142	9-Jun-06	140km/h 20 min								passive regeneration
194	9-Jun-06	5x80 km/h 20 min								steady state
344	12-Jun-06	2x80km/h 20 min								steady state
404	12-Jun-06	120km/h 20 min		0.48	0.009	0.22	0.046	0.21	167.2	preconditioning
448	12-Jun-06	3xEUDC		1.21	0.009	0.22	0.061	0.21	162.2	preconditioning
469	13-Jun-06	NEDC	4.7E+10	0.96	0.014	0.52	0.145	0.50	191.9	EUDC regeneration
481	13-Jun-06	120km/h 20 min								preconditioning (regeneration)
44	13-Jun-06	2x80km/h 20 min								steady state
104	13-Jun-06	3 EUDC								preconditioning
125	14-Jun-06	NEDC	1.6E+11	0.94	0.011	0.15	0.082	0.14	158.1	Insatallation of new filtering system. Not working properly
202	15-Jun-06	NEDC	9.9E+10	0.81	0.010	0.22	0.080	0.21	160.8	Insatallation of new filtering system. Not working properly
279	16-Jun-06	NEDC	6.6E+10	0.86	0.011	0.22	0.085	0.21	161.1	Insatallation of new filtering system. Not working properly
356	19-Jun-06	NEDC	4.5E+10	0.68	0.011	0.22	0.085	0.20	159.4	Insatallation of new filtering system. Not working properly
433	20-Jun-06	NEDC	4.6E+10	0.85	0.010	0.22	0.071	0.21	161.7	Insatallation of new filtering system. Not working properly
510	21-Jun-06	NEDC	5.1E+10	0.81	0.010	0.23	0.085	0.22	160.1	Insatallation of new filtering system. Not working properly
587	22-Jun-06	NEDC	3.9E+10	0.89	0.011	0.22	0.081	0.21	159.6	Insatallation of new filtering system. Not working properly
664	23-Jun-06	NEDC	6.9E+10	0.64	0.010	0.23	0.074	0.22	162.2	Insatallation of new filtering system. Not working properly
741	26-Jun-06	NEDC	8.3E+10		0.022	0.82	0.264	0.80	181.7	Insatallation of new filtering system. Not working properly
829	3-Jul-06	NEDC1	6.9E+09	0.66	0.011	0.28	0.073	0.21	160.1	cold morning test
840	4-Jul-06	NEDC2	9.4E+09	0.55	0.011	0.27	0.082	0.18	160.2	cold morning test
851	4-Jul-06	NEDC3	8.1E+08	0.45	0.004	0.23	0.014	0.22	151.0	hot
862	4-Jul-06	NEDC4	1.4E+09							hot after lunch no preconditioning
873	4-Jul-06	NEDC5	1.5E+09							hot no preconditioning
884	4-Jul-06	NEDC6	1.4E+09							hot no preconditioning
895	5-Jul-06	NEDC7	2.5E+10							cold morning test no preconditioning
906	5-Jul-06	NEDC8	6.9E+08							hot no preconditioning
917	5-Jul-06	NEDC9	7.6E+08							hot no preconditioning
928	5-Jul-06	NEDC10	8.9E+09	0.57						hot afternoon test no preconditioning
939	5-Jul-06	NEDC11	1.1E+09	0.45						hot no preconditioning
950	5-Jul-06	NEDC12	1.1E+09	0.38						hot no preconditioning
961	6-Jul-06	NEDC13	7.5E+09	0.62						cold morning test no preconditioning
972	6-Jul-06	NEDC14	6.5E+08	0.60						hot no preconditioning
	6-Jul-06	NEDC15	4.0E+09	1.05						hot no preconditioning
	6-Jul-06	NEDC16	6.1E+10	0.79						hot afternoon test no preconditioning
	6-Jul-06	NEDC17	2.8E+09	0.66						hot no preconditioning
	7-Jul-06	NEDC18	1.5E+11	0.47						cold morning test no preconditioning
	7-Jul-06	NEDC19	3.6E+09	21.65						hot no preconditioning
	7-Jul-06	NEDC20	3.7E+09	0.55						hot no preconditioning
	10-Jul-06	NEDC21	5.4E+10	0.45						cold morning test no preconditioning
	10-Jul-06	NEDC22	2.1E+09	0.45						hot no preconditioning
11	10-Jul-06	NEDC23	1.6E+11	0.51						hot afternoon test no preconditioning
	11-Jul-06	120 km/h		0.96						
83	12-Jul-06	NEDC24	1.7E+11	0.47						cold morning test
	13-Jul-06	120 km/h								
155	14-Jul-06	NEDC25	4.1E+10	0.32						cold morning test
		NEDC26		0.43						

European Commission

EUR 22311 EN – Joint Research Centre, Institute for the Environment and Sustainability

Title: PMP Inter-laboratory Correlation Exercise: Report on Part 3: JRC Tests in July'06

Authors: Barouch Giechaskiel, Rafael Muñoz-Bueno, Rinaldo Colombo, Urbano Manfredi, Panagiota Dilara

Luxembourg: Office for Official Publications of the European Communities

2007 – 44 pp. – 21 x 29.9 cm

EUR - Scientific and Technical Research series; ISSN 1018-5593

Abstract

This document reports the results of the third part of the testing performed during the PMP inter-laboratory exercise - 13 July to 18 August 2006 - conducted at the Vehicles Emissions Laboratory (VELA2) in the Transport and Air Quality Unit of the European Commission's Joint Research Centre (JRC-Ispra). This report presents the results of the work undertaken on a 2.0 HDi diesel car equipped with a Diesel Particulate Filter (DPF), i.e. the Golden Vehicle. Most of the tests complied with all the requirements of the document UN-GRPE PMP Phase 3. Inter-laboratory Correlation Exercise: Framework and Laboratory Guide. The measurements included both filter based particulate mass measurements and real-time particle number measurements performed under transient conditions on a chassis dynamometer. Extra tests were conducted in order to investigate the effect of the PMP recommendations over the legislated procedures (filter media, temperature, cyclone, no backup filter). Moreover the regeneration emissions were investigated. Finally comparisons with the previous measurements of the same vehicle in JRC were made.

Mission of the JRC

The mission of the JRC is to provide customer-driven scientific and technical support for the conception, implementation and monitoring of EU policies. As a service of the European Commission, the JRC functions as a reference centre of science and technology for the Union. Close to the policy-making process, it serves the common interest of the Member States, while being independent of special interests, whether private or national.

